Isomerism of Complexes Containing Thiourea Dianion Ligands

A thesis submitted in partial fulfilment
of the requirements for the degree
of
Master of Science
in Chemistry
at
The University of Waikato
by

Jane Estelle Spenceley

The University of Waikato
2014

THE UNIVERSITY OF
WAIKATO
Te Whare Wānanga o Waikato

Abstract

This thesis reports the synthesis and characterisation of eight new platinum thiourea complexes. Thiourea dianion complexes of the type $(Ph_3P)_2PtSC(=NR)NPh$, R=Me, Et, Pr^n, Pr^i, Bu^n and $(Ph_3P)_2PtSC(=NPh)NR$ R=Bu^t, *p*-tol, and the thiourea monoanion complex of the type $[(Ph_3P)_2PtSC(=NEtH)NPh]^+$ were synthesised. This research confirms the prediction made by Henderson *et al* that asymmetrically substituted thiourea dianion complexes could form isomers. NMR studies show that the kinetically favoured isomer is formed initially, and then undergoes a solution phase isomerisation process to form the thermodynamically favoured isomer. Evidence that this isomerisation is affected by difference in substituent size and the energy difference between the two structures was obtained both experimentally, by use of NMR spectroscopy techniques, and theoretically using DFT calculations. Theoretically optimised geometries of each isomer allowed the calculation of $\Delta G(GPt_{rem}\text{-}GPt_{adj})$ for each pair. NMR techniques were used to monitor the isomerisation process, which was clearly visible in both ^1H and ^{31}P spectra. The relative substituent size, difference in energy between the two structures and rate of isomerisation appear to be proportional to each other. The greater the substituent size difference, the greater the difference in energy and faster the rate of isomerisation from the kinetically favoured isomer to the thermodynamically favoured isomer.

Acknowledgements

First on this list are my two excellent supervisors, who, although very different were both absolutely irreplaceable. Professor Bill Henderson, thank you for letting me run wild with this project, for finding me something that incorporated everything I love in chemistry and more. I hope I didn't stray too far from what you intended the outcomes to be. Dr Joseph Lane, thank you for always believing in me, for your support and encouragement, it got me to where I am today.

Half of the discoveries could not have been made without the expertise of Professor Alistair Wilkins; thank you for being so patient and so willing to help me with anything related to NMR. I couldn't have done it without you.

Wendy Jackson, without your assistance I would probably still be looking for chemicals and equipment. Thank you to all the technicians, I am forever grateful to all of you for letting me invade your labs to use equipment and steal chemicals and glassware, I promise I always put them back...

Jess and Sophie thank you for being with me on this journey. If I hadn't had such awesome friends to go through all of the pain and suffering with I wouldn't have enjoyed it anywhere near as much. Words can't even explain how many thank yous need to go to everyone in the Chemistry Department, the people I met and the friends I made along the way. You are all amazing.

To The Bandies, The Theatre Crowd, there are too many of you to name and guaranteed I have forgotten someone but all of you need to be thanked for putting up with me and my chemistry. I know I didn't make a lot of sense but thank you for letting me rant at you when I needed it, and only telling me to "shut up with the science" half the time.

Kristy and Shane, what on earth would I have done without you both. I can't even explain how much your support meant to me. Thank you for accepting my crazy and just rolling with it.

Katie, the lab coat you bought me for my 17th birthday was the best present ever! Thank you for being there for the last 15 years, for helping me with my assignments and occasionally asking me a question in a lab and making me feel super brainy.

Thank you to all the amazing and inspirational role models I had growing up. My high school chemistry teacher Mr McHale your passion and dedication to education and science started me on this path. All my high school teachers, thank you for believing in me.

The de Langes and the Halliwells, thank you for the support and the advice, you have both been second families to me. Words cannot sum up how much I appreciate everything.

Mum and Dad, absolutely none of this would have been possible without you. Thank you isn't a big enough word for what you have done. Thank you for being amazing parents, for letting me try everything, for giving me amazing opportunities, for supporting me no matter what. Thank you for visiting me in Hamilton and doing all my laundry and making me food and doing my shopping. Thank you for supporting and encouraging me throughout this process, even though half the time you had no idea what I was ranting about. I love you both so much. Thank you for everything you have done for me, I couldn't have done it without you.

Table of Contents

List of Figures

List of Tables

List of Abbreviations

NMR - nuclear magnetic resonance spectroscopy

IR - infrared spectroscopy

ES-MS - electrospray mass spectrometry

δ - chemical shift ppm (NMR)

m/z - mass to charge ratio (ES-MS)

s - singlet (NMR), strong (IR)

d - doublet (NMR)

t - triplet (NMR)

qt – quintet (NMR)

m - multiplet (NMR), medium (IR)

w – weak (IR)

J - coupling constant in Hz (NMR)

DFT - Density functional theory

$CDCl_3$ – Deuterated chloroform

COD - Cyclooctadiene

DPPE - 1,2-bis(diphenylphosphino)ethane

DPPF - 1,2-bis(diphenylphosphino)ferrocene

HIV - human immunodeficiency virus

HDL - high-density lipoprotein

HSAB - hard soft acid base theory

Pt_{rem} - The isomer where the R group is attached to the nitrogen remote to platinum

Pt_{adj} - The isomer where the R group is attached to the nitrogen directly bonded to platinum

ΔG - The difference in Gibbs free energy between Pt_{rem} and Pt_{adj} isomers

Chapter 1 Introduction

Thioureas are well known and versatile organosulfur compounds of the formula $SC(NR^1R^2)(NR^3R^4)$ (Figure 1.1). They are easily derivatised and a wide range of differently substituted examples are known. In a 1954 review Schroeder tabulated over 1000 known substituted thioureas of the types $RHNCSNH_2$, $RR'NCSNH_2$, $(RNH)_2CS$, $RHNCSNHR'$, $RR'NCSNHR''$ and S substituted varieties [1]. R groups include both alkyl- and aryl- type substituents, ranging from the most simple methyl and phenyl groups to complicated long chain and substituted aryl groups. Thioureas have a wide range of uses in both industrial and pharmaceutical applications, which stems from the ability to tune both the electronic and steric properties by varying R group substitution. It is clear from this review that even 60 years ago thioureas were recognised as incredibly versatile chemicals, and much research since has focused on their properties in both chemical and biological systems.

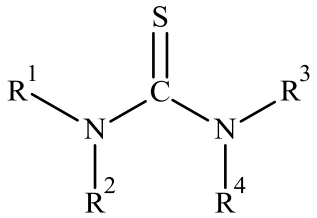

Figure 1.1 General structure of thiourea illustrating substitutable R group positions

In chemical systems thiourea itself is most commonly used in the preparation of thiourea dioxide, $(NH)(NH_2)CSO_2H$ (Figure 1.2), which is used for reductive bleaching in the textiles industry [2], as well as leaching gold and silver ores and in

diazo blueprint papers. Other applications include use as a photographic toning agent, in hair preparations and in the production of synthetic resins [3].

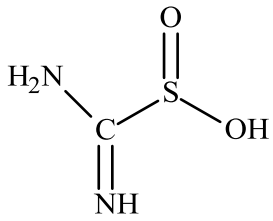

Figure 1.2 Molecular structure of thiourea dioxide

In biological systems thioureas present a broad range of activities including anti-HIV (human immunodeficiency virus), anti-cancer, anti-viral, analgesic, anti-bacterial and HDL-elevating (high-density lipoprotein) [4-7]. Acyl thioureas in particular are known for their bactericidal, fungicidal, herbicidal and insecticidal modes of action, and have been used to regulate plant growth [8], however, the potency of these activities is highly influenced by substituent choice.

Thioureas are also able to act as ligands towards metal centres. Their combination of soft sulfur and hard nitrogen atoms allows them to bind to a wide variety of metal centres including, but not limited to, platinum, palladium, molybdenum, nickel [9], ruthenium and rhodium [10]. The description of sulfur as “soft’ and nitrogen as “hard” derives from Pearson’s Hard Soft Acid Base theory (HSAB) [11]. A soft base is characterised by a large radius, neutral or negative charge and the ability to be easily polarised. A hard base is characterised by small ionic radus, high electronegativity and weakly polarisable. Pearson states that soft acids will form their stronger complexes with soft bases. Conversely, hard acids will form their stronger complexes with hard bases [12]. Platinum is defined as a soft acid,

and so by HSAB theory it is expected to have a higher affinity to sulfur, a soft base, rather than to nitrogen, a hard base.

Thiourea binding as a monodentate neutral ligand is the most commonly observed coordination mode, and a large number of examples are known. In this mode the thiourea coordinates through the sulfur, which, as a "soft" donor, has a higher affinity for the soft metals than the "hard" nitrogen. Figure 1.3 shows an example of thiourea coordinating through sulfur as a monodentate ligand. [13-15]

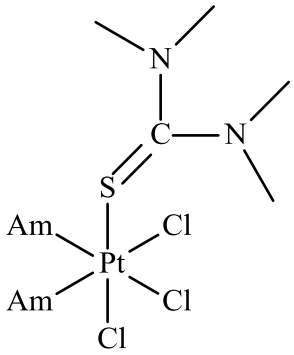

Figure 1.3 Examples of monodentate S coordination to platinum metal, Am=amine

1.1 Other coordination modes of thioureas

Thioureas are also known to bind as mono- and di-anions (Figure 1.4). These often coordinate as bidentate chelating ligands to the metal centre, forming four-membered MSCN rings. Instances of the monoanion complex are more frequent than the dianion.

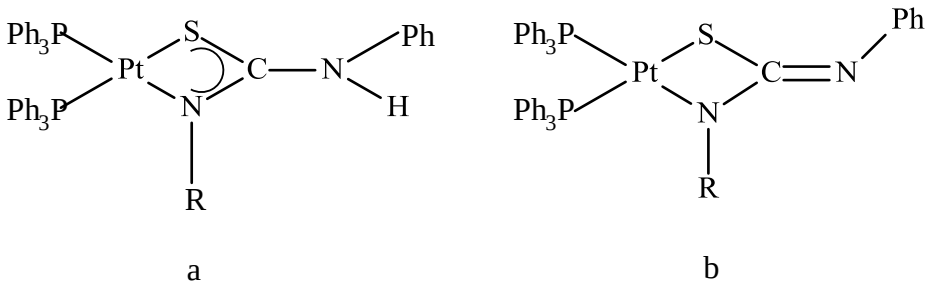

Figure 1.4 Examples of the structure of a thiourea monoanion (a), and thiourea dianion (b) complexes, both coordinated as bidentate ligands

1.1.1 Synthesis and structure of thiourea dianion complexes

The first reported complex of a thiourea dianion was a bis(triphenylphosphine) platinum(II) complex with a N,N'-diethylthiourea dianion coordinated as an N,S-chelating ligand [16]. This complex was synthesised by the addition of an equimolar amount of N,N'-diethylthiourea to a solution of $[Pt(acac)(PPh_3)_2](acac)$ in methanol. $(Ph_3P)_2PtSC(=NEt)NEt$ (Figure 1.5) was isolated as yellow cubic crystals in a 60% yield.

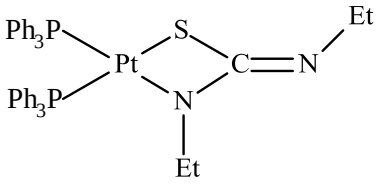

Figure 1.5 Structure of $(Ph_3P)_2PtSC(=NEt)NEt$ [16]

In the same year a second group reported the synthesis and structure of $(Ph_3P)_2PtSC(=NPh)NPh$. [17] This synthesis used two equivalents of triphenylphosphine, followed by one equivalent of N,N'-diphenylthiourea and an excess of silver(I) oxide added in succession to a stirred solution of $[PtCl_2(cod)]$ in dichloromethane, giving a pale yellow crystalline solid. Figure 1.6 shows the X-ray crystal structure of this compound. The four membered PtSCN ring is approximately planar, and the two phenyl groups sit at right angles to the plane of the ring. Complexes containing thiourea dianion ligands are uncommon and the two examples described above are two of only four reported in the Cambridge Crystallographic database [18,19].

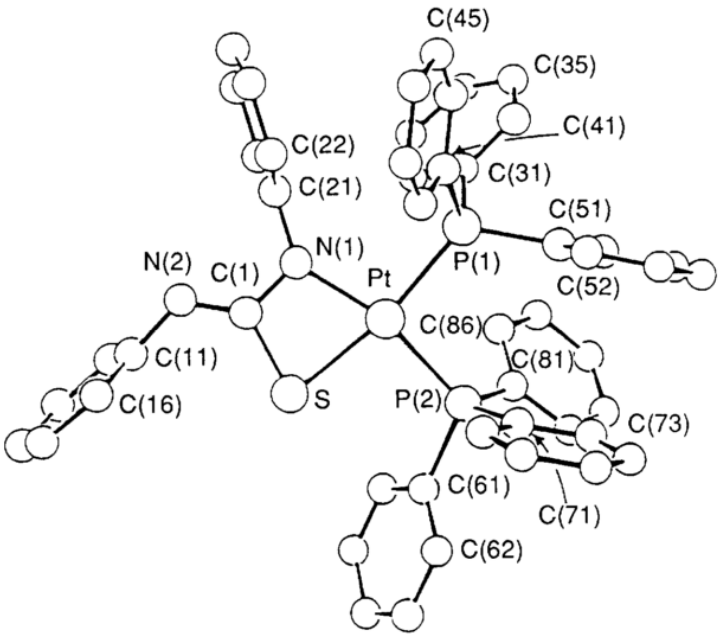

Figure 1.6 X-ray crystal structure of $(Ph_3P)_2PtSC(=NPh)NPh$ [17]

Thiourea dianion complexes were next reported in the literature when in 1993 Pilato *et al* reported the synthesis of a molybdenum compound with the same ligand structure, [19] in this case the synthesis was quite different in that di-*p*-tolylcarbodiimide was added into the molybdenum sulfido bond (Figure 1.7).

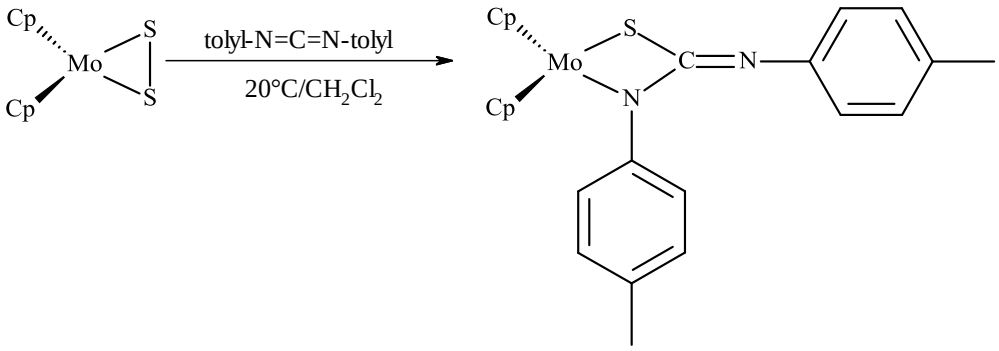

Figure 1.7 Reaction scheme and structure of $Cp_2MoSC(=N\text{-}tolyl)N\text{-}tolyl$ $Cp=\eta^5\text{-}C_5H_5$ [19]

Figure 1.8 shows an example of an asymmetrically substituted thiourea coordinated to platinum as a dianion. This compound was synthesised by Henderson *et al* with a variety of ligands, L. For example the compound with L = PPh_3 was synthesised from a mixture of $PtCl_2(PPh_3)_2$ and the sodium salt of 1-cyano-3-methylisothiourea in methanol with excess triethylamine. [18]

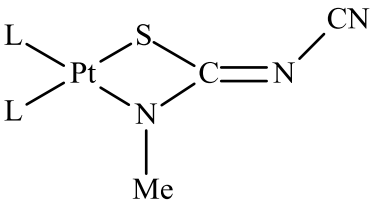

L = PPh_3, PBu^n_3, $P(OPh)_3$
L-L = COD, DPPE, DPPF

Figure 1.8 Asymmetric thiourea dianion ligand coordinated bidentate to platinum [18]

1.1.1.1 Complexes containing selenourea dianion ligands

The first complex containing a chelating selenourea dianion ligand was reported in 2003 (Figure 1.9). It was synthesised from a mixture of *cis*-$PtCl_2(PPh_3)_2$ and N,N'-diphenylselenourea with triethylamine, the same method used for the majority of platinum thiourea complexes. Another common method for the thiourea complex synthesis uses silver oxide as a base. The attempted synthesis of the selenourea complex using silver(I) oxide in place of triethylamine as the base gave a large number of unidentified products, presumed to be products of the oxidation of selenium by silver. [20]

To date no other examples of a selenourea coordinating in this manner have been reported, possibly due to the odorous nature of the ligands precursors and the difficulty involved with handling them.

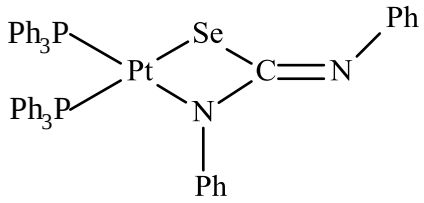

Figure 1.9 First example of a complex of a selenourea dianion ligand showing bidentate coordination to platinum [20]

1.1.2 Synthesis and structure of thiourea monoanion complexes

Thiourea monoanion complexes have been reported for a wide range of metals. A small representation of the range of different compounds currently reported in the literature is given below.

Platinum examples of thiourea monoanions have been reported. Henderson *et al* reported the synthesis and structures of a number of compounds, Figure 1.10 shows a selection, synthesised by reaction of *cis*-$PtCl_2(PPh_3)_2$ and the appropriate thiourea with excess triethylamine followed by addition of $NaBPh_4$. [13]

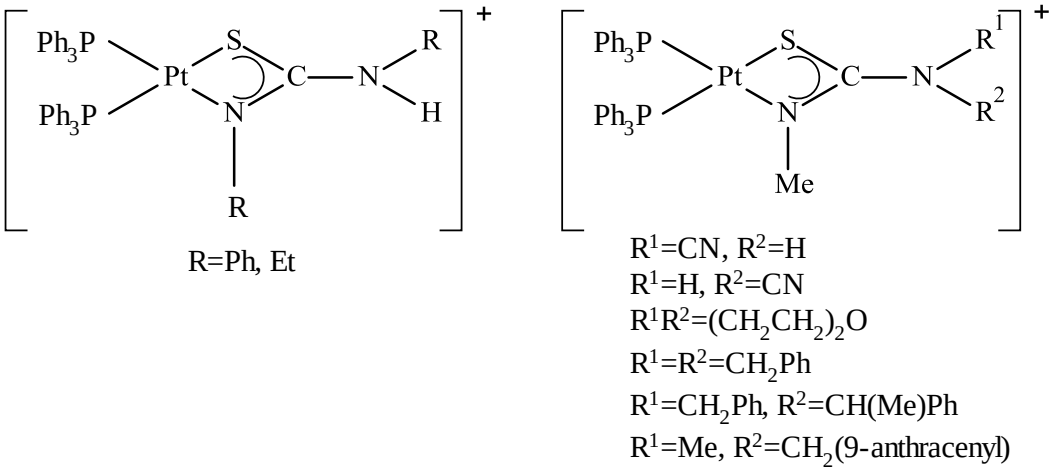

Figure 1.10 Some platinum complexes of thiourea monoanion ligands [13]

Tris(N,N'-diphenylthioureato)chromium(III) was reported in 1992. This compound contains three chelating thiourea monoanions all coordinated to Cr(III) (Figure 1.11). This compound was synthesised from a solution of $Cr(CO)_6$ and $SC(NHPh)_2$ in THF (tetrahydrofuran). [21]

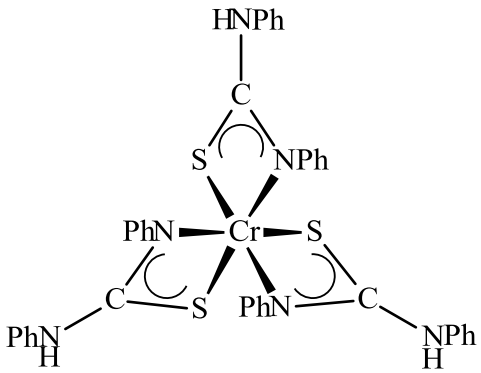

Figure 1.11 Structure of tris(N,N'-diphenylthioureato)chromium(III) [21]

Thiourea monoanion ligands have also been reported coordinated to aluminium [22], the compounds form via a methane elimination reaction of $AlMe_3$ with di-substituted thioureas Figure 1.12.

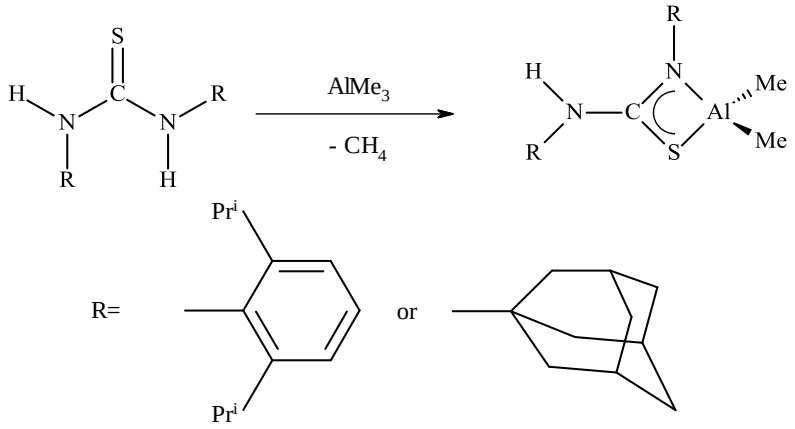

Figure 1.12 Reaction scheme showing the formation of {R'HNC(NR')S}$AlMe_2$ by methane elimination and the structures of the two R' groups used [22]

Ruthenium thiourea monoanion complexes were also reported using $NaBPh_4$ as the precipitating agent. A mixture of $[(\eta^6\text{-cym})RuCl_2]_2$, Ph_3P, $PhNHC(S)NMe_2$, and Et_3N were refluxed in MeOH after which $NaBPh_4$ was added to the hot mixture. This method gave the yellow solid $[Ru(\eta^6\text{-cym})(PPh_3)\{\kappa^2N,S\text{-}PhNC(S)NMe_2\}]BPh_4$ (Figure 1.13). [23]

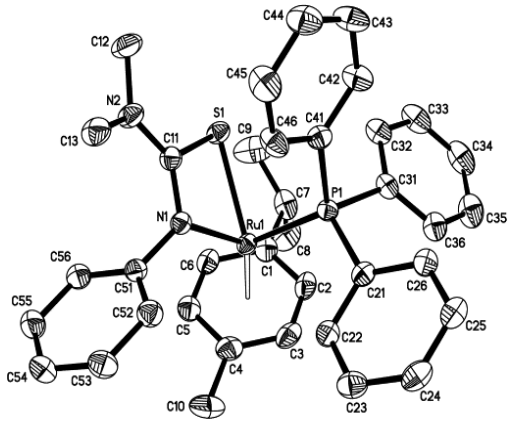

Figure 1.13 Crystal structure of the thiourea monoanion complex $[Ru(\eta^6\text{-cym})(PPh_3)\{\kappa^2\text{-}N,S\text{-}PhNC(S)NMe_2\}]BPh_4$ [23]

Robinson *et al* reported the synthesis of N,N'-diphenylthiourea complexes of ruthenium, osmium and iridium [24]. In each of these compounds the thiourea coordinates bidentate as a monoanion forming a MSCN ring with the metal centre. The structures reported are shown in Figure 1.14.

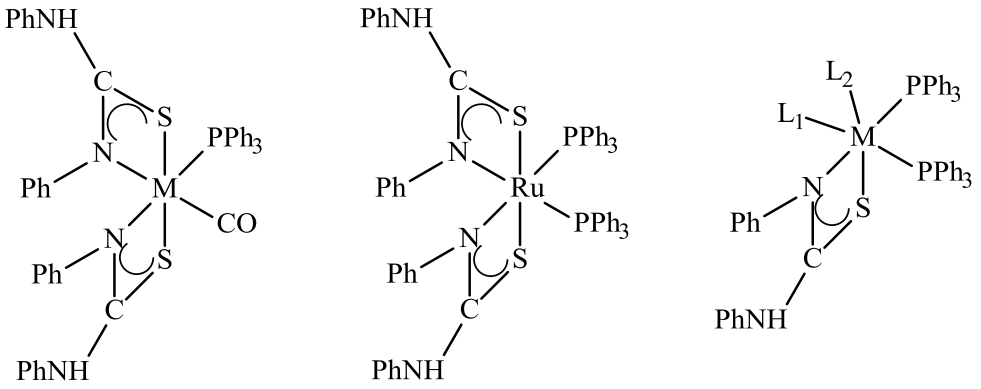

1 2 3, 4, 5

1 M=Ru, Os
3 M=Ru, L_1=H, L_2=CO
4 M=Ru, L_1=Cl, L_2=CO
5 M=Ir, L_1=H, L_2=H

Figure 1.14 Thiourea monoanions coordinated to ruthenium, osmium and iridium as bidentate ligands [24]

Figure 1.15 shows the structure of a nickel monoanion complex and a nickel bis(monoanion) complex reported in 2011 [9]. The monoanion complex was synthesised with a range of R substituents, given in Table 1.1. Another monoanion complex which contained two bidentate monoanion thioureas was also reported (Figure 1.15b).

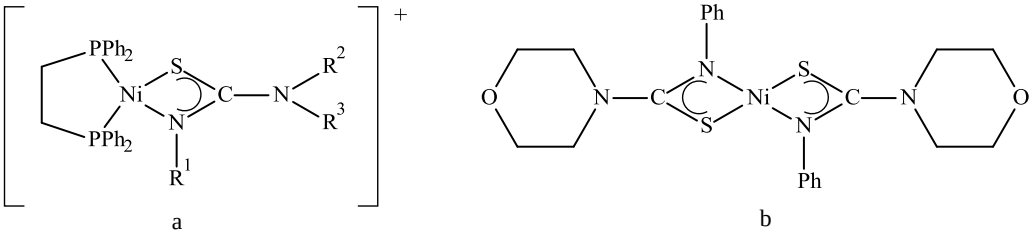

Figure 1.15 Nickel thiourea monoanion complexes [9]

Table 1.1 The different R substituent combinations that have been reported for the nickel monoanion complex shown in Figure 1.15a

R^1	R^2,R^3
Ph	Me, Me
Ph	Cy, Cy
Ph	$(CH_2)_4$
Ph	$(CH_2)_5$
Ph	$(CH_2CH_2)_2O$
Ph	$(CH_2CH_2)_2S$
Ph	CH_2Ph, (R)-CHMePh
Ph	Ph, H
Bu^n	Bu^n, H
p-$C_6H_4NO_2$	Me, Me
p-$C_6H_4NO_2$	$(CH_2CH_2)O$

Most recently Smith *et al* reported gold thiourea monoanion complexes, with a variety of substituents. These were synthesised *via* the common triethylamine route and $NaBPh_4$ was added after refluxing. This precipitated the monoanion complex from a mixture of an organo gold chloride complex, the appropriate thiourea and triethylamine [25]. The compounds reported are given in Figure 1.16.

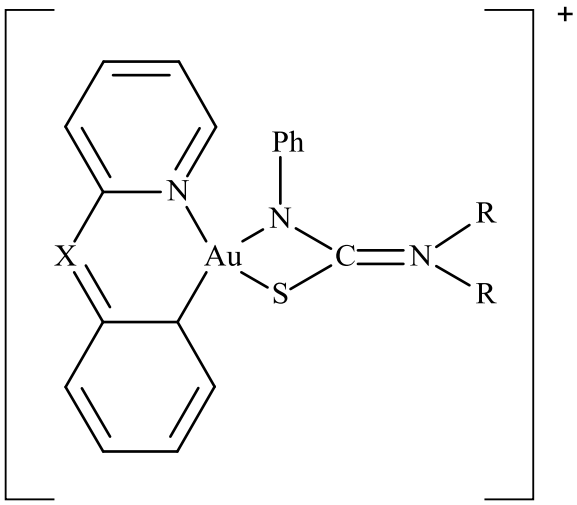

a X = NH, R = Cy
b X = NH, R = Me
c X = CH_2, R = Me
d X = NH, RR = $(CH_2CH_2)_2O$

Figure 1.16 Gold thiourea monoanion complexes reported by Smith *et al*. [25]

1.2 Thiosemicarbazide complexes

Thiourea and thiosemicarbazides are structurally very similar, the only difference being the thiosemicarbazide has an additional nitrogen atom. Figure 1.17 shows the structures of the two ligands.

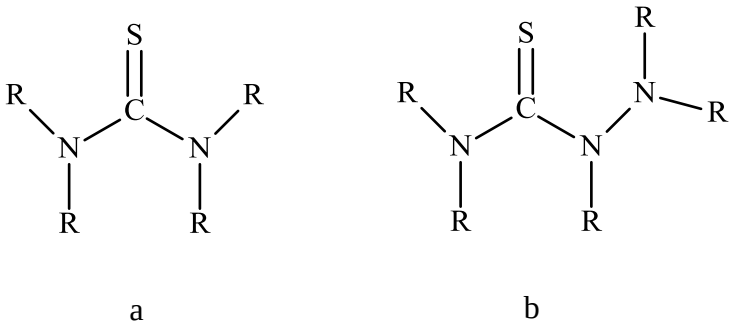

Figure 1.17 Structural comparison of thiourea (a) and thiosemicarbazide (b)

These two ligands are also known to bind in similar ways to metals. Both will coordinate bidentate forming a four membered MSCN ring.

A paper by Henderson *et al* reported the first thiosemicarbazide bonded to a transition metal as a dianion ligand. The compound was synthesised by the addition of Et_3N to a stirred mixture of *cis*-$[PtCl_2(PPh_3)_2]$ and a slight excess of $Ph_2NNHC(S)NHPh$, in MeOH, immediately giving the bright yellow $(Ph_3P)_2PtSC(=NPh)NNPh_2$. NMR spectroscopy provided evidence that two isomers are present in the sample. $(Ph_3P)_2PtSC(=NPh)NNPh_2$ (Figure 1.18a) showed the expected AB pattern from $^{31}P\{^1H\}$ NMR, corresponding to two inequivalent PPh_3 ligands coordinated to platinum. Phosphine resonances occurred at δ 16.9 and 11.1 showing $^1J(PtP)$ coupling constants of 3156 and 3147 Hz respectively. As well as these major signals there appeared to be a minor species in the isolated product with approximately 5% intensity. This product also followed the AB pattern as above with ^{195}Pt coupling of 3038 and 3330 Hz, which is consistent with N and S donor ligands. As the electrospray mass spectrometry

(ES MS) spectrum showed a single $[M+H]^+$ ion for the crude product the minor signals were assigned to an isomeric structure as shown in Figure 1.18b.

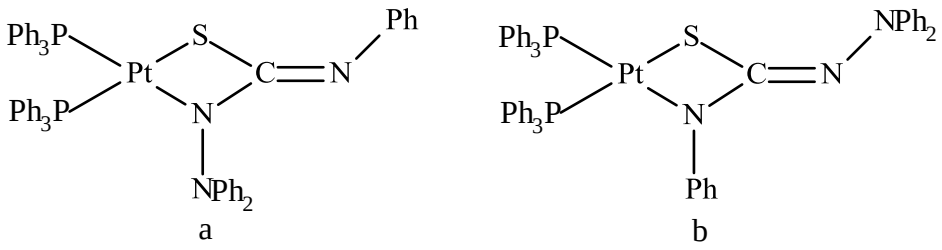

Figure 1.18 Isomers formed by the 1,1,4-triphenyl thiosemicarbazide ligand when coordinated to platinum [21]

Of the two isomers formed, the major structure (Figure 1.18a) appears to form preferentially because there is less steric bulk adjacent to the platinum coordination system with the NPh_2 group on the nitrogen adjacent to the platinum, as evident from the crystal structure in Figure 1.19.

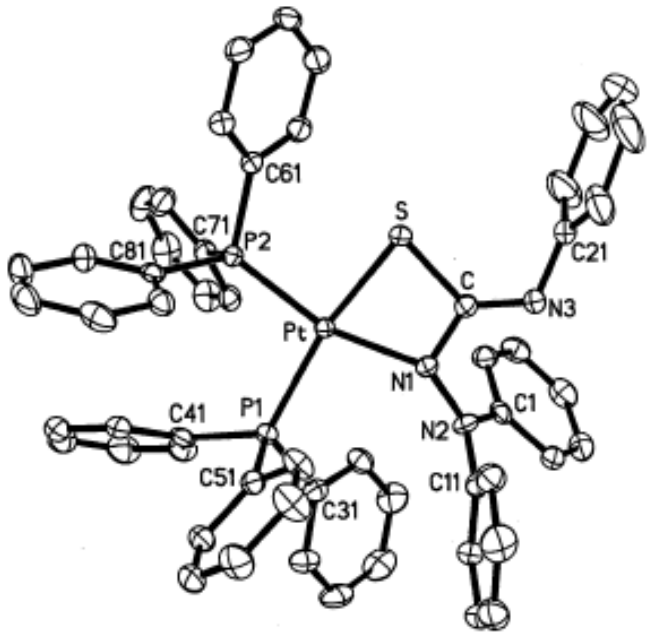

Figure 1.19 Crystal structure of $[Pt\{SC(=NPh)NNPh_2\}(PPh_3)_2]$ showing the major isomer [21]

To test this reasoning the large phenyl group was replaced by a sterically less bulky methyl group, following the same synthesis but replacing the $Ph_2NNHC(S)NHPh$ with $Ph_2NNHC(S)NHMe$. The result was the complex shown in Figure 1.20, with the opposite isomer dominant compared to the triphenyl compound. The Pt-NMe group was readily assigned in the ^{1}H NMR spectrum at δ 2.43, this signal showed coupling to both ^{31}P (4.1 Hz) and ^{195}Pt (29.9 Hz).

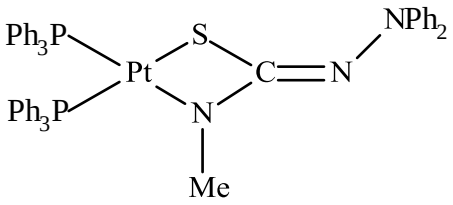

Figure 1.20 Structure of the major product when the Ph substituent of $[Pt\{SC(=NPh)NNPh_2\}(PPh_3)_2]$ is replaced by the smaller Me group, forming $[Pt\{SC(=NMe)NNPh_2\}(PPh_3)_2]$

Structurally the thiosemicarbazide ligands are similar to the thiourea ligands; both forming the same membered MSCN rings. This paper postulated that the analogous thiourea ligands could also form substituent dependant isomers [26].

To date the literature does not contain any information pertaining specifically to isomerisation in thiourea dianion complexes. This thesis addressed that gap and provides some insight into the formation of these isomers.

1.3 Thesis overview

Thioureas that are substituted with different groups can potentially form two different structures when they coordinate bidentate to a metal centre. The two structures will henceforth be described as Pt_{adj}, where the R substituent is bonded to the nitrogen adjacent to the platinum (Figure 1.21a), and Pt_{rem}, where the R substituent is bonded to the nitrogen remote to the platinum (Figure 1.21b). The second substituent of both isomers will be Ph, due to the synthetic method used.

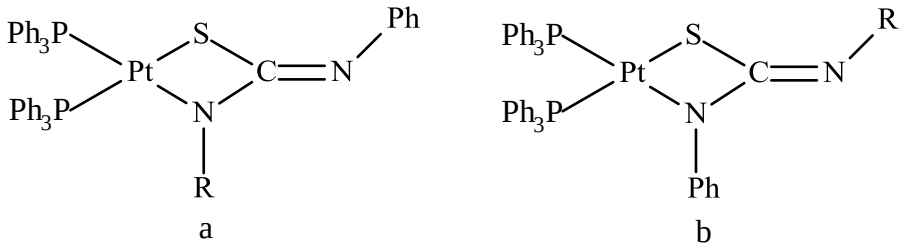

Figure 1.21 Possible isomers of compounds with different R substituents on the thiourea ligand a=Pt_{adj}, b=Pt_{rem}.

To date the majority of thiourea dianion complexes reported are symmetrically substituted RNH-C(=S)-NHR, and the small number of asymmetric thioureas R^1NH-C(=S)-NHR^2 have not been the focus of isomer investigations. In particular the previously mentioned $(Ph_3P)_2$PtSC(=NCN)NMe (Section 1.2) has the potential to form isomers (Figure 1.22a/b). The reported NMR data contains only one set of signals, so only one isomer was made. This can be identified as the Pt_{adj} isomer, R=Me, from the evidence of $^3J_{Pt\text{-}H}$ coupling (Figure 1.22c) on the NMe group of approximately 31 Hz. If the Pt_{rem} isomer was present there would not be any Pt-H coupling present.

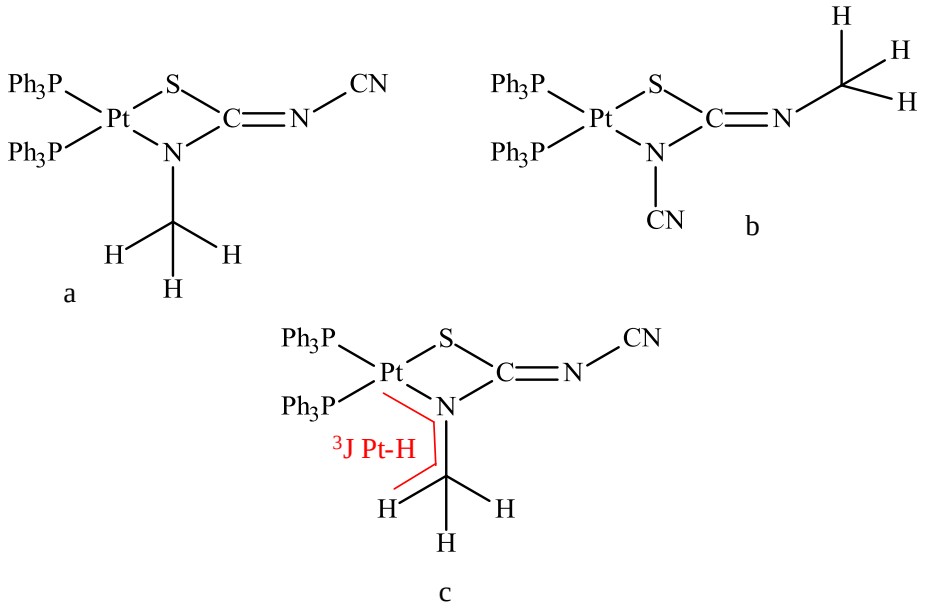

Figure 1.22 a) Pt_{adj} isomer, b) Pt_{rem} isomer, c) illustration of Pt-H coupling in the Pt_{adj} isomer

This thesis focuses on the formation of structural isomers in platinum compounds containing thiourea dianions. Substituents are limited to phenyl-alkyl mixtures as alkyl groups are sufficiently different to Ph groups and provide a distinct spectroscopic 'handle' as well as the ease by which they are synthesised.

Substituted thioureas are easily synthesised by the reaction shown in Figure 1.23. The use of PhNCS was convenient as it is commercially available, inexpensive and forms crystalline thioureas with a range of different amines.

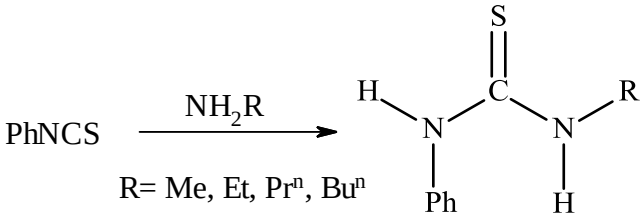

Figure 1.23 Reaction scheme for the synthesis of substitued thioureas from phenylisothiocyanate and primary amines

Isomers of thiourea dianion complexes will form when the energy barrier between the different isomer structures is low. Assuming that the two structures are in thermal equilibrium the population of each state can be determined by a Boltzmann distribution. As the energy gap widens it becomes increasingly more likely that only the lower energy structure will form to any appreciable amount.

There are a number of factors that can influence the formation of isomers if the system has not reached thermal equilibrium. The inherent energy difference between the two isomers can be affected by solid state and solvent effects. Solid state effects influence the packing of molecules into unit cells, a structure can distort from its solution phase form into a more favourable crystal packing arrangement. The solute, in this case the platinum compound, must occupy cavities created between the solvent molecules. It is possible that one of the isomers will have more solute-solvent interactions that are more favourable than the other isomer. This favourability will lead to one of the isomers being more stable in the solvent than the other and this isomer will have the greater population when dissolved. For these effects to be easily compared a range of phenyl-alkyl combinations have been chosen. Straight chain alkyl groups Me, Et, Pr^n and Bu^n and non-straight chain alkyls Pr^i, and Bu^t provide a good range of steric bulk from small to very large.

The alkyl groups are easily identifiable by proton NMR spectroscopy, as they are the only signals in the aliphatic region of the spectrum. It is expected that $^3J_{Pt\text{-}H}$ coupling will be observed in the n-alkyls from the Pt_{adj} isomer but not the Pt_{rem}, so the two will be easily distinguished for this group of compounds. The non-straight chain alkyl compounds will rely more heavily on theoretical calculations to distinguish between the two isomers, as Pt-H coupling will not be observed for

either isomer due to the structure of the alkyl substituent. *p*-tol was also used in combination with Ph to provide a steric size match while still maintaining asymmetric substitution.

Thiourea dianion complexes syntheses are commonly reported by a triethylamine method or a silver(I) oxide method in the literature. Of these two syntheses the triethylamine method is chosen. This is due to evidence that the silver(I) oxide method produces unidentified by-products [26], whereas the triethylamine method produces pure compounds. Figure 1.24 shows the reaction scheme used for all the platinum complexes synthesised.

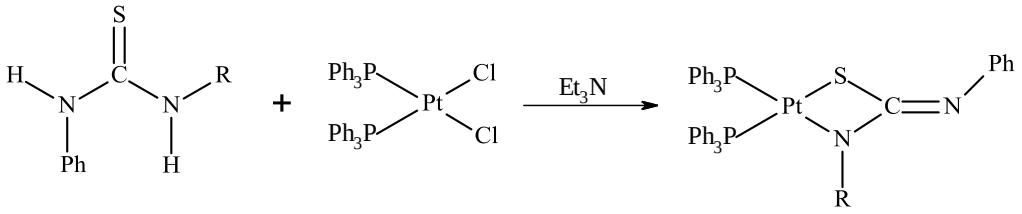

Figure 1.24 Triethylamine reaction scheme used for the synthesis of compounds in this thesis, showing (for simplicity) only the Pt_{adj} isomer as the product

Chapter 2 General synthetic, spectroscopic and theoretical methods

Thioureas PhNHC(S)NHR R=Me, Pr^n, Pr^i, Bu^t, were prepared in high yields by the addition of the appropriate primary amine to a solution of PhNCS (Aldrich) in diethyl ether and stirring until a suspension of white crystalline product is obtained (Figure 2.1). Thioureas PhNHC(S)NHR R=Et, Bu^n, *p*-tol, were previously prepared laboratory samples, synthesised by the same method.

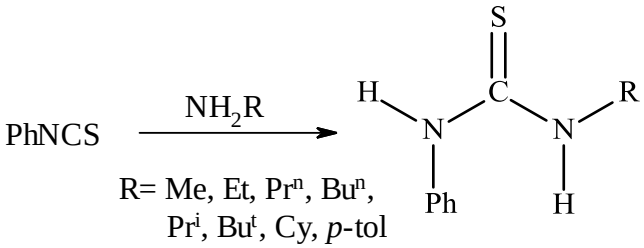

Figure 2.1 Reaction scheme for the synthesis of substituted thioureas from phenyl isothiocyanate and primary amines

To synthesise $(Ph_3P)_2PtCl_2$ a 2 mole equivalent of PPh_3 was added to a stirred suspension of $CODPtCl_2$ in dichloromethane and stirred for 5 minutes. Petroleum spirit was added to complete precipitation. The resulting white solid was filtered and washed with petroleum spirit before being dried under vacuum. Figure 2.2 shows the reaction scheme. $CODPtCl_2$ was synthesised using literature methods [27].

$$CODPtCl_2 + 2PPh_3 \longrightarrow (Ph_3P)_2PtCl_2 + COD$$

COD = Cyclo-octadiene

Figure 2.2 Reaction scheme for the synthesis of $(Ph_3P)_2PtCl_2$ from $CODPtCl_2$

Elemental analyses of all compounds were performed by the Campbell Microanalytical Laboratory, Department of Chemistry, University of Otago. ES MS were recorded in positive ion mode on a Bruker microTOF instrument, in methanol solvent. Calibration was carried out using a solution of sodium formate. Infrared spectra were recorded as KBr disks on a Perkin Elmer Spectrum 100 Fourier Transform IR spectrometer, with a wavenumber range of 4000-400 cm^{-1}. Raman spectra were recorded as pure powders on a PerkinElmer RamanStation 400 spectrometer, from 95 – 3500 cm^{-1} Raman shift. The excitation source was a 350 mW near-infrared 785 nm laser, delivering 100 mW at the sample. $^{31}P\{^{1}H\}$ and ^{1}H NMR spectra were recorded on a Bruker AVANCE(III) 400 MHz instrument in $CDCl_3$ solution at 300K. Melting Points were recorded on a Reichert-Jung thermovar as solid samples placed on glass slides.

2.1 Theoretical methods

Density functional theory (DFT) calculations were carried out using Gaussian 2009 [28] on the University of Waikato's high performance computing cluster Symphony.

Initial input geometries were constructed using the known crystal structure of $(Ph_3P)_2PtSC(=NPh)NPh$ as a template. The thiourea R groups were then substituted with Me, Et, Pr^n, Pr^i, Bu^n, Bu^t and *p*-tol in both the adjacent and remote positions. All DFT calculations were completed with the M06-2X density functional using the 6-311++G(2d,2p) basis set for all main group elements and the LANL2DZ basis set and effective core potential for platinum. This level of theory was found to have the highest congruency with the bond lengths and angles of the $(Ph_3P)_2PtSC(=NPh)NPh$ crystal structure, as shown in Appendix 1. Geometry optimisations and harmonic frequency calculations were run with the

default criteria. The geometries were also reoptimised in the presence of an implicit solvent using the IEFPCM method. The solvent optimised geometries were then used to calculate NMR chemical shifts with the GIAO method, also in the presence of an implicit solvent. The reference NMR shifts for TMS were also obtained using the M06-2X/6-311++G(2d,2p) level of theory with the GIAO method in the presence of an implicit solvent.

2.2 Synthesis and characterisation of platinum complexes containing substituted thiourea dianion ligands

This section reports the synthesis and characterisation of complexes containing a thiourea dianion ligand substituted with n-alkyl groups Et, Me, Pr^n, Bu^n, branched alkyl groups Pr^i and Bu^t, and the aromatic group *p*-tol.

2.2.1 Synthesis

Equimolar amounts of *cis*-$PtCl_2(PPh_3)_2$ and PhNHC(S)NHR were suspended in methanol (25 mL) in a 100 mL round bottom flask with a magnetic stirrer and refluxed for 5 min resulting in a pale yellow clear solution. Et_3N (0.1 mL) was then added and the resulting mixture refluxed (refer to Table 2.1 for specific times) resulting in a clear pale yellow solution. Distilled water (70 mL) was added and the suspension cooled to room temperature. The resulting yellow precipitate was filtered on a Büchner funnel, washed successively with cold distilled water (2x10 mL) and diethyl ether (3 mL), and then dried under vacuum. N.B. 0.2g of NaCl was added to the $(Ph_3P)_2$PtSC(=NMe)NPh suspension, coagulating the precipitate for ease of filtration. Details pertaining to each compound specifically are given in Table 2.1.

Table 2.1 Specific synthesis conditions for the platinum complexes containing substituted thiourea dianion ligands

R	PhNHC(S)NHR		$(Ph_3P)_2PtCl_2$		Reflux time (X)	Yield
	mg	mmol	mg	mmol	min	mg, %
Et	24.8	0.138	102.6	0.13	15	95.3, 82%
Me	26.8	0.163	123.2	0.156	20	92.0, 67 %
Pr^n	27.3	0.128	101.3	0.14	20	76.3, 65%
Bu^n	26.6	0.131	100.4	0.127	15	66.1, 57%
Pr^i	26.7	0.137	101.6	0.128	30	104.2, 89%
Bu^t	27.1	0.131	103.8	0.133	25	72.1, 59%
p-tol	37	0.153	115.3	0.146	15	82.7, 59%

2.2.2 Characterisation

Note in all ES-MS only the $[M+H]^+$ ion was present and the ^1H NMR only report characterising peaks; the aromatic region is of little interest due to the complexity of signals arising from the two triphenylphosphine groups.

2.2.2.1 $(Ph_3P)_2PtSC(=NEt)NPh$

Elemental Analysis: Found (%) C 59.63, H 4.49, N 3.13. Calculated (%) C 60.19, H 4.49, N 3.12.

Melting point: 244-288 ^{0}C.

ES-MS: Theoretical *m/z* 898.211. The *m/z* for the positive $[M+H]^+$ ion was found to be 898.427.

FTIR: initial precipitate, Pt_{rem}: 3053 (w), 1662 (w), 1597 (s), 1578 (s), 1482 (m), 1436 (s), 1384 (m), 1339 (w), 1301 (m), 1211 (w), 1175 (w), 1097 (s), 1070 (w),

1047 (w), 1027 (w), 999 (w), 949 (w), 843 (w), 796 (w), 749 (m), 693 (s), 643 (w), 615 (w), 547 (m), 525 (s), 512 (m), 495 (m).

Solid from evaporation of NMR sample in $CDCl_3$, Pt_{adj}: 3052 (w), 1681 (w), 1598 (m), 1545 (s), 1481 (m), 1435 (s), 1384 (w), 1314 (w), 1206 (m), 1096 (s), 998 (w), 920 (w), 743 (m), 693 (s), 546 (s), 526 (s), 516 (s), 498 (s).

RAMAN: Al plate, cm^{-1} (initially formed product, Pt_{rem}): 3058 (s), 3042 (m), 1587 (s), 1577 (m), 1445 (w), 1304 (m), 1099 (m), 1032 (m), 1001 (s), 691 (w), 618 (m), 370 (m), 277 (w), 258 (m).

Al plate, cm^{-1} (Solid from evaporation of NMR sample in $CDCl_3$, Pt_{adj}): 3055 (s), 1585 (s), 1538 (s), 1486 (m), 1439 (m), 1357 (m), 1096 (m), 1030 (m), 1001 (s), 687 (w), 619 (m), 366 (w), 277 (w), 257 (m).

NMR: Pt_{rem}: $^{31}P\{^1H\}$ δ 15.9 ppm [$^1J_{(PtP)}$ 3129 Hz, $^2J_{(PP)}$ 17 Hz] and δ 11.4 ppm [$^1J_{(PtP)}$ 3257 Hz, $^2J_{(PP)}$ 17 Hz]. ^1H δ 3.19 ppm [q, CH_2, $^3J_{(HH)}$ 7.1 Hz] and δ 1.0 ppm [t, CH_3, $^3J_{(HH)}$ 7.2 Hz].

Pt_{adj}: $^{31}P\{^1H\}$ δ 18.7 ppm [$^1J_{(PtP)}$ 3077 Hz, $^2J_{(PP)}$ 21 Hz] and δ 13.6 ppm [$^1J_{(PtP)}$ 3145 Hz, $^2J_{(PP)}$ 21 Hz]. ^1H δ 2.98 ppm [m, CH_2, $^3J_{(PtH)}$ 46 Hz] and δ 0.50 ppm [t, CH_3, $^3J_{(HH)}$ 6.8 Hz].

2.2.2.2 $(Ph_3P)_2PtSC(=NMe)NPh$

Elemental Analysis: Found (%) C 58.20, H 4.32, N 3.20. Calculated (%) C 59.79, H 4.33, N 3.17.

Melting Point: 238-246^{0}C.

ES-MS: Theoretical *m/z* 884.196. The *m/z* for the positive $[M+H]^+$ ion was found to be *m/z* 884.203.

FTIR: initial precipitate: 3052 (w), 1599 (w), 1554 (s), 1481 (m), 1436 (m), 1402 (w), 1384 (w), 1330 (w), 1208 (w), 1095 (m), 1026 (w), 998 (w), 894 (w), 744 (w), 693 (s), 618 (w), 547 (m), 526 (m), 516 (m), 499 (w).

NMR: Pt_{rem}: $^{31}P\{^{1}H\}$ δ 16.0 ppm and δ 11.5 ppm. Unable to observe satellite peaks for this isomer, ^{1}H δ 2.83 ppm [s, CH_3].

Pt_{adj}: $^{31}P\{^{1}H\}$ δ 18.0 ppm [$^{1}J_{(PtP)}$ 3072 Hz, $^{2}J_{(PP)}$ 20 Hz] and δ 13.9 ppm [$^{1}J_{(PtP)}$ 3166 Hz, $^{2}J_{(PP)}$ 20 Hz], ^{1}H δ 2.47 ppm [m, CH_3, $^{3}J_{(PtH)}$ 34 Hz, $^{4}J_{(PH)}$ 4 Hz].

2.2.2.3 $(Ph_3P)_2PtSC(=NPr^n)NPh$

Elemental Analysis: Found (%) C 60.63, H 4.63, N 3.11. Calculated (%) C 60.58, H 4.64, N 3.07.

Melting Point: 230-238^{0}C.

ES-MS: Theoretical *m/z* 912.227. The *m/z* for the positive $[M+H]^+$ ion was found to be *m/z* 912.253.

FTIR: initial precipitate: 3051 (w), 2955 (w), 2928 (w), 2867 (w), 1599 (s), 1580 (s), 1482 (m), 1435 (s), 1384 (m), 1281 (w), 1158 (w), 1096 (s), 1066 (w), 743 (m), 693 (s), 618 (w), 547 (m), 525 (s), 515 (m), 498 (m).

NMR: Pt_{rem}: $^{31}P\{^{1}H\}$ δ 16.9 ppm [$^{1}J_{(PtP)}$ 3103 Hz, $^{2}J_{(PP)}$ 22 Hz] and δ 12.2 ppm [$^{1}J_{(PtP)}$ 3187 Hz, $^{2}J_{(PP)}$ 22 Hz]. ^{1}H δ 3.1 ppm [t, CH_2, $^{3}J_{(HH)}$ 7.3 Hz], δ 1.4 ppm [m, CH_2, $^{3}J_{(HH)}$ 7.5 Hz] and δ 0.8 ppm [t, CH_3, $^{3}J_{(HH)}$ 7.3 Hz].

Pt_{adj}: $^{31}P\{^{1}H\}$ δ 19.0 ppm [$^{1}J_{(PtP)}$ 3075 Hz, $^{2}J_{(PP)}$ 20 Hz] and δ 13.7 ppm [$^{1}J_{(PtP)}$ 3132 Hz, $^{2}J_{(PP)}$ 20 Hz]. ^{1}H δ 2.8 ppm [m, CH_2, $^{3}J_{(PtH)}$ 44 Hz], δ 1.2 ppm [m, CH_2, $^{4}J_{(PtH)}$ 38 Hz] and δ 0.05 ppm [t, CH_3, $^{3}J_{(HH)}$ 7.3 Hz].

2.2.2.4 $(Ph_3P)_2PtSC(=NBu^n)NPh$

Elemental Analysis: Found (%) C 60.80, H 4.68, N 3.07. Calculated (%) C 60.56, H 4.80, N 3.03.

Melting Point: 240-243^{0}C.

ES-MS: ES-MS: Theoretical *m/z* 926.242. The *m/z* for the positive $[M+H]^+$ ion was found to be *m/z* 926.264.

FTIR: initial precipitate: 3418 (m), 3051 (w), 2955 (w), 2924 (w), 2857 (w), 1601 (s), 1581 (m), 1482 (m), 1435 (m), 1384 (m), 1344 (w), 1279 (m), 1160 (w), 1096 (m), 1069, 1028 (w), 999 (w), 744 (w), 692 (s), 547 (m), 525 (s), 513 (m), 497 (m).

NMR: Pt_{rem}: $^{31}P\{^1H\}$ δ 16.5 ppm [$^1J_{(PtP)}$ 3110 Hz, $^2J_{(PP)}$ 22 Hz] and δ 11.9 ppm [$^1J_{(PtP)}$ 3218 Hz, $^2J_{(PP)}$ 22 Hz]. ^1H δ 3.1 ppm [t, CH_2, $^3J_{(HH)}$ 7.3 Hz], δ 1.4 ppm [m, CH_2, $^3J_{(HH)}$ 7.2 Hz], δ 1.2 ppm [m, CH_2, $^3J_{(HH)}$ 7.6 Hz] and δ 0.8 ppm [t, CH_3, $^3J_{(HH)}$ 7.3 Hz]

Pt_{adj}: $^{31}P\{^1H\}$ δ 18.9 ppm [$^1J_{(PtP)}$ 3074 Hz, $^2J_{(PP)}$ 21 Hz] and δ 13.7 ppm [$^1J_{(PtP)}$ 3130 Hz, $^2J_{(PP)}$ 21 Hz]. ^1H δ 2.8 ppm [m, CH_2, $^3J_{(PtH)}$ 50 Hz], δ 1.1 ppm [m, CH_2, $^4J_{(HH)}$ unresolved], δ 1.2 ppm [m, CH_2, $^3J_{(HH)}$ unresolved] and δ 0.39 ppm [s, CH_3, $^3J_{(HH)}$ unresolved].

2.2.2.5 $(Ph_3P)_2PtSC(=NPr^i)NPh$

Elemental Analysis: Found (%) C 59.33, H 4.73, N 3.05. Calculated (%) C 60.58, H 4.64, N 3.07.

Melting Point: 228-234^{0}C.

ES-MS: Theoretical *m/z* 912.227. The *m/z* for the positive $[M+H]^+$ ion was found to be *m/z* 912.244.

FTIR: initial precipitate: 3054 (w), 2958 (w), 2860 (w), 1594 (s), 1569 (s), 1481 (m), 1435 (s), 1385 (w), 1337 (w), 1289 (w), 1140 (w), 1097 (s), 1027 (w), 998 (w), 747 (m), 693 (s), 617 (w), 547 (m), 525 (s), 515 (m), 499 (m).

NMR: Pt_{rem}: $^{31}P\{^{1}H\}$ δ 16.8 ppm [$^{1}J_{(PtP)}$ 3093 Hz, $^{2}J_{(PP)}$ 23 Hz] and δ 12.3 ppm [$^{1}J_{(PtP)}$ 3189 Hz, $^{2}J_{(PP)}$ 22 Hz]. ^{1}H δ 3.7 ppm [m, CH, $^{3}J_{(HH)}$ 6.3 Hz] and δ 1.0 ppm [d, CH_3, $^{3}J_{(HH)}$ 6.6 Hz]

Pt_{adj}: $^{31}P\{^{1}H\}$ δ 20.0 ppm [$^{1}J_{(PtP)}$ 3073 Hz, $^{2}J_{(PP)}$ 21 Hz] and δ 14.0 ppm [$^{1}J_{(PtP)}$ 3096 Hz, $^{2}J_{(PP)}$ 22 Hz]. ^{1}H δ 3.8 ppm [m, CH, $^{3}J_{(HH)}$ 5.8 Hz], δ 1.0 ppm [m, CH_2, $^{4}J_{(HH)}$ 6.5 Hz].

2.2.2.6 $(Ph_3P)_2PtSC(=NBu^t)NPh$

Elemental Analysis: Found (%) C 60.15, H 4.77, N 3.01. Calculated (%) C 60.96, H 4.79, N 3.03.

Melting Point: 201-204^{0}C.

ES-MS: Theoretical *m/z* 926.242. The *m/z* for the positive $[M+H]^+$ ion was found to be *m/z* 926.277.

FTIR: initial precipitate: 3414 (w), 3050 (w), 2965 (w), 2943 (w), 2917 (w), 1662 (w), 1597 (s), 1577 (s), 1480 (m), 1434 (m), 1352 (w), 1281 (m), 1281 (m), 1135 (w), 1096 (s), 1072 (w), 998 (w), 980 (w), 741 (m), 693 (s), 545 (m), 525 (s), 514 (s), 499 (m).

NMR: Pt_{rem}: $^{31}P\{^{1}H\}$ δ 13.3 ppm [$^{1}J_{(PtP)}$ 3179 Hz, ^{2}J(PP) 21 Hz] and δ 9.2 ppm [$^{1}J_{(PtP)}$ 3441 Hz, $^{2}J_{(PP)}$ 22 Hz]. ^{1}H δ 1.39 ppm [s].

Pt_{adj}: $^{31}P\{^{1}H\}$ δ 17.6 ppm [$^{1}J_{(PtP)}$ 3059 Hz, ^{2}J(PP) 22 Hz] and δ 12.4 ppm [$^{1}J_{(PtP)}$ 3154 Hz, $^{2}J_{(PP)}$ 22 Hz]. ^{1}H δ 1.38 ppm [s]

2.2.2.7 $(Ph_3P)_2PtSC(=N\textit{p}\text{-tol})NPh$

Elemental Analysis: Found (%) C 62.36, H 4.45, N 3.05. Calculated (%) C 62.56, H 4.41, N 2.91.

Melting Point: 205-216^{0}C, 219-224^{0}C, the stable mixture of two isomers results in two different melting point ranges.

ES-MS: Theoretical *m/z* 960.227. The *m/z* for the positive $[M+H]^+$ ion was found to be *m/z* 960.264.

FTIR: initial precipitate: 3053 (w), 2920 (w), 1593 (s), 1554 (s), 1504 (m), 1482 (m), 1436 (m), 1384 (w), 1311 (w), 1234 (w), 1185 (w), 1097 (m), 999 (w), 818 (w), 744 (m), 693 (s), 618 (w), 545 (m), 525 (m), 516 (m), 497 (w).

NMR: Isomer A $^{31}P\{^1H\}$ δ 16.71 ppm [$^1J_{(PtP)}$ 3081 Hz, $^2J(PP)$ 21 Hz] and δ 11.83 ppm [$^1J_{(PtP)}$ 3230 Hz, $^2J_{(PP)}$ 22 Hz]

Isomer B $^{31}P\{^1H\}$ δ 16.74 ppm [$^1J_{(PtP)}$ 3081 Hz, $^2J(PP)$ 21 Hz] and δ 11.76 ppm [$^1J_{(PtP)}$ 3230 Hz, $^2J_{(PP)}$ 22 Hz]

Pt_{rem} ^1H δ 1.9 ppm [s]

Pt_{adj} ^1H δ 2.2 ppm [s].

Chapter 3 Platinum complexes containing asymmetrical thiourea dianion ligands substituted with n-alkyl groups

This chapter contains discussion on the solution phase isomerisation of these compounds, and reports evidence supporting kinetic and thermodynamic products as a cause of this phenomenon. $(Ph_3P)_2PtSC(=NEt)NPh$ is discussed first in detail as the isomerisation process was initially observed in NMR experiments on this compound. For ease of distinction between compounds they will henceforth be described as L_{PhR}, defining them by the R group substituent on the thiourea ligand. All compounds were synthesised by the scheme illustrated in Figure 3.1.

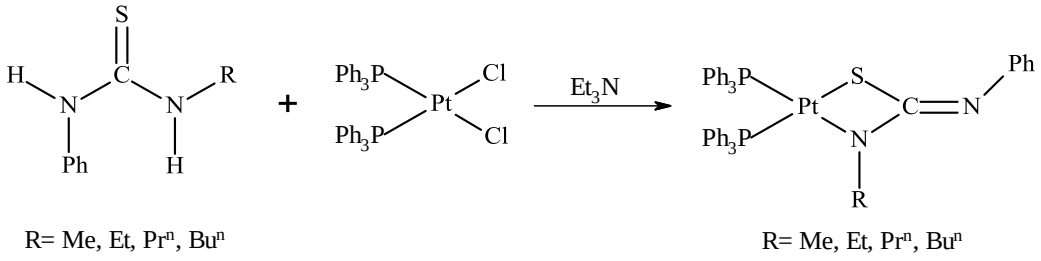

Figure 3.1 Reaction scheme illustrating the synthesis of platinum complexes containing n-alkyl substituted thiourea dianion ligands

3.1 $(Ph_3P)_2PtSC(=NEt)NPh$ (L_{PhEt})

L_{PhEt} was synthesised from a mixture of *cis*-$PtCl_2(PPh_3)_2$ and EtNHC(S)NHPh with Et_3N in methanol. On the addition of water to the hot reaction mixture a yellow solid was precipitated, $(Ph_3P)_2PtSC(=NEt)NPh$. ES-MS data showed a pure compound, with the dominant Pt isotope peak for the $[M+H]^+$ ion at *m/z*=897.91. ES-MS cannot detect the presence of isomers but does prove that this

sample was pure. To make predictions about whether or not isomers will form, theoretical calculations were carried out. Based on Gibbs free energy differences between the two isomers ($\Delta G(GPt_{rem}\text{-}GPt_{adj})$) the more stable isomer will be lower in energy; a positive $\Delta G(GPt_{rem}\text{-}GPt_{adj})$ value implies that Pt_{adj} is favoured. NMR studies were carried out in $CDCl_3$ to fully characterise and determine if isomers were present. The results are as follows.

Theoretical calculations showed that the difference in free energy between the Pt_{adj} and Pt_{rem} isomers (Figure 3.2) is 21 kJ mol^{-1} ($\Delta G(GPt_{rem}\text{-}GPt_{adj})$); Pt_{adj} was lower in energy than Pt_{rem} by this amount. Assuming thermal equilibrium and a Boltzmann distribution this energy difference corresponds to the Pt_{adj} isomer being >99% abundant at room temperature. On this basis it is assumed that only one isomer, Pt_{adj}, will be synthesised.

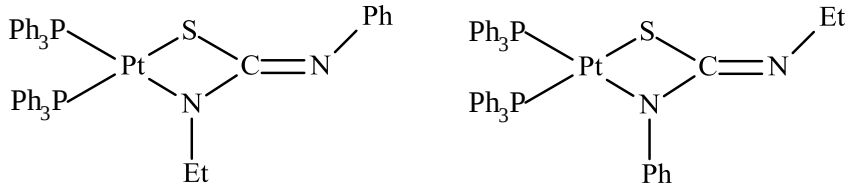

Figure 3.2 Structures of Pt_{adj} (a) and Pt_{rem} (b), the potential isomers formed by $(Ph_3P)_2PtSC(=NEt)NPh$

3.1.1 NMR investigation

All ^1H NMR spectra discussed in this section are limited to the alkyl region, as the aromatic region is of no significant interest to this investigation. '*' indicate unidentified impurity peaks.

Initial experimental NMR spectra showed signals that indicated the presence of only one isomer, in apparent agreement with the theoretical predictions. The proton NMR spectrum, as presented in Figure 3.4 top, showed the quartet and triplet signals that would be expected from the presence of an ethyl group. However, the quartet signal showed no platinum coupling, indicating that the R group is remote from the platinum (Figure 3.2b). This is not the isomer that was predicted to be dominant by theoretical calculations.

As platinum couplings are observed as small peaks on the edges of the main signals, it was initially thought that the couplings could be hidden in the baseline. A second spectrum was run on the same sample aimed at improving the signal to noise ratio and increasing the resolution.

At the time the second proton spectrum was recorded the sample had been in the NMR solvent, $CDCl_3$, for several hours. It became clear during analysis that in the few hours between the two scans the sample had changed, as evidenced by comparison of the spectrum in Figure 3.3 and Figure 3.4.

The quartet in Figure 3.4 clearly shows platinum coupling, shown expanded in Figure 3.5, leading to the conclusion that over time the compound has isomerised into the structure predicted to be theoretically dominant, Pt_{adj}, with the R group adjacent to the platinum. The upfield shift of the quartet and triplet signals, caused by the proximity to the electron rich platinum, also indicates that the Et group is closer to the platinum.

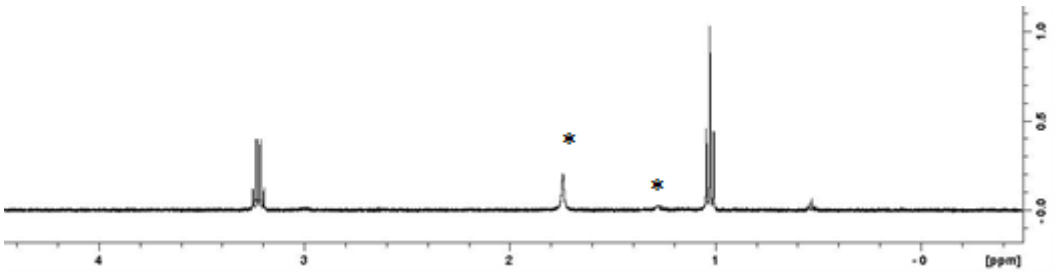

Figure 3.3 ^{1}H NMR spectrum of $(Ph_3P)_2PtSC(=NEt)NPh$ in $CDCl_3$, after 5 minutes. * = unidentified

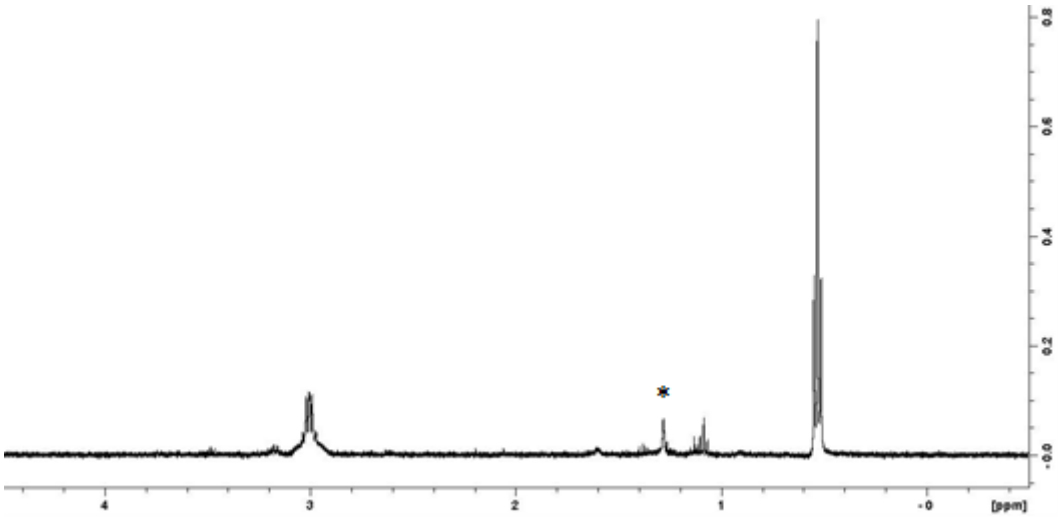

Figure 3.4 ^{1}H NMR spectrum from the same batch of $(Ph_3P)_2PtSC(=NEt)NPh$ in $CDCl_3$, after 3 hours in the solvent, showing the first indication of isomerisation from Pt_{rem} into Pt_{adj}. * = unidentified

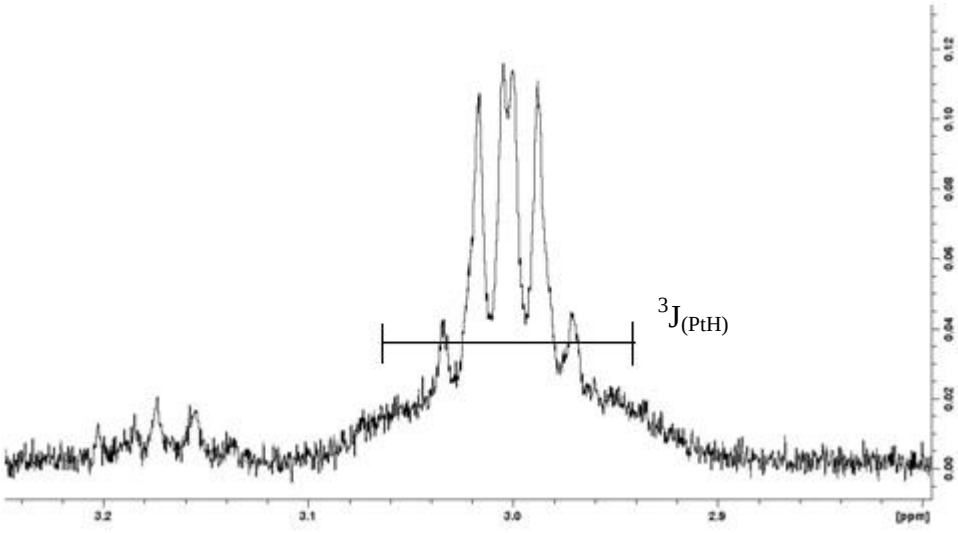

Figure 3.5 Expansion if the δ 3.0 ppm quartet showing Pt-H coupling

The free ligand PhHNC(S)NHEt has the same ^{1}H quartet/triplet pattern at similar chemical shifts, δ 3.68 ppm and δ 1.2 ppm. The observed shift in the quartet and triplet signals could be attributed to free ligand coordinating to platinum in the NMR sample tube, however, ESI-MS of the initially formed product rules this out as the only observed *m/z* value matched the theoretical *m/z* for the $[M+H]^{+}$ ion of the thiourea complex. To further investigate the cause of this chemical shift change more NMR experiments were carried out. A new sample was made and data collection started almost immediately after its dissolution in $CDCl_3$. This sample was monitored with a number of sequential short ^{1}H spectra until isomerisation was complete, a period of approximately 90 minutes for this compound.

The first ^{1}H NMR spectrum, Figure 3.6, recorded after approximately 5 minutes showed a quartet at 3.2 ppm, and a triplet at 1.0 ppm, corresponding to the CH_2 and CH_3 groups of the ethyl respectively. No platinum coupling was observed on the quartet peak, consistent with Pt_{rem} (Figure 3.2b). This spectrum has a very small second triplet at 0.5 ppm, but no clear second quartet peak.

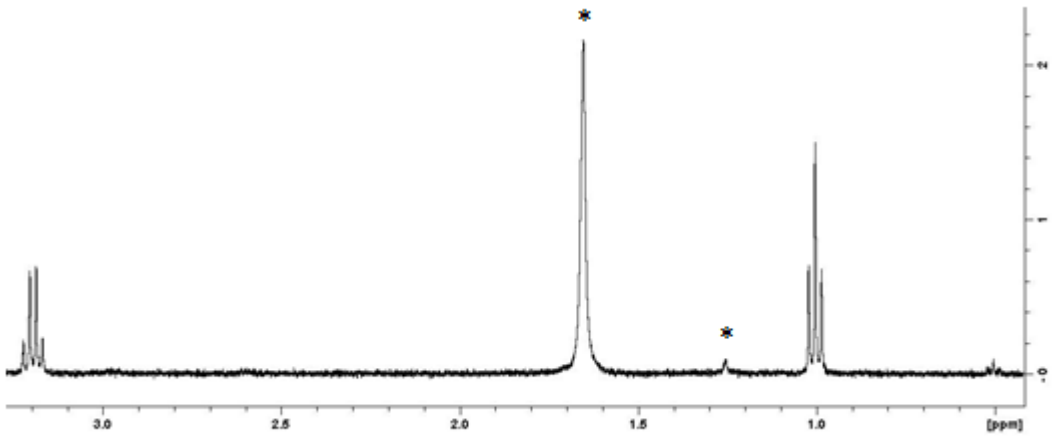

Figure 3.6 ^{1}H spectrum of $(Ph_3P)_2PtSC(=NEt)NPh$ after 5 minutes in $CDCl_3$ solution. * = unidentified

After 45 minutes, shown in Figure 3.7, the smaller signals at 2.9 ppm and 0.5 ppm had grown, now distinctly a quartet and a triplet, and the previously dominant peaks had shrunk to approximately equal intensities. The 2.9 ppm quartet peak showed Pt coupling, Figure 5.4 expansion, which gave evidence that this pair of signals belonged to the Pt_{adj} isomer.

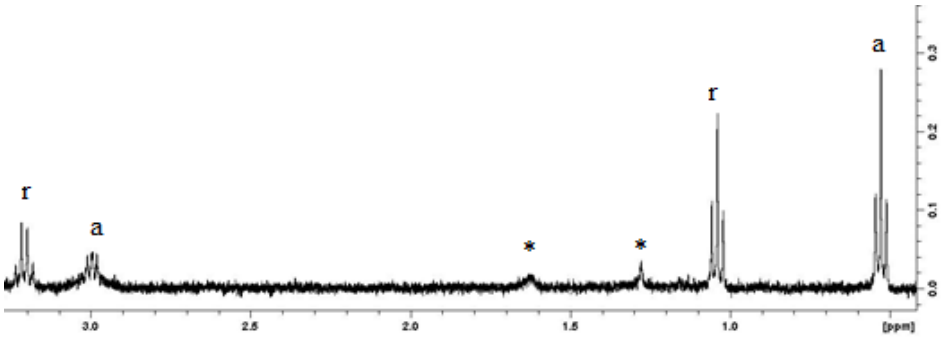

Figure 3.7 ^{1}H spectrum of $(Ph_3P)_2PtSC(=NEt)NPh$ after 45 minutes in $CDCl_3$ solution. Both isomers are now clearly visible. a and r indicate Pt_{adj} and Pt_{rem} isomers respectively. * = unidentified

Figure 3.8 shows the ^{1}H spectrum after 90 minutes, the original quartet and triplet signals (3.2 ppm and 1.0 ppm) had almost entirely disappeared and the previously barely visible signals (2.9 ppm and 0.5 ppm) now dominated the spectrum.

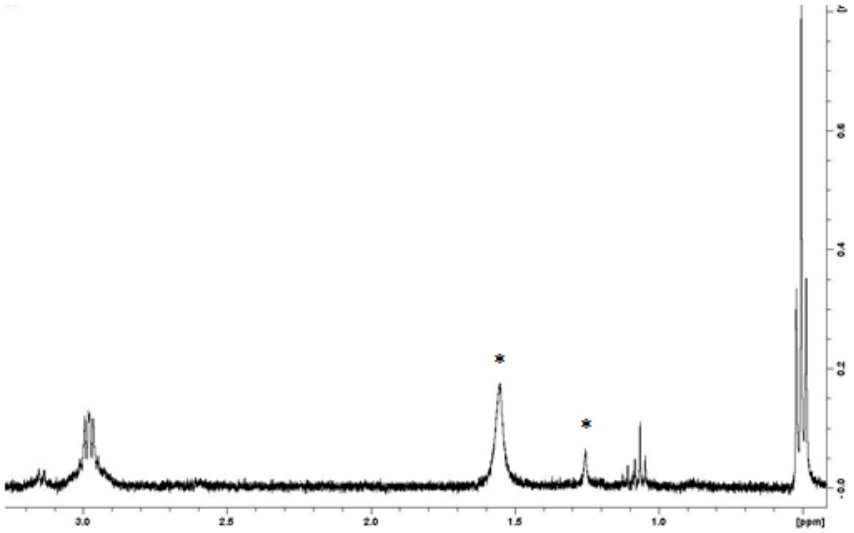

Figure 3.8 ^{1}H spectrum of $(Ph_3P)_2PtSC(=NEt)NPh$ after 90 minutes in $CDCl_3$ solution. The Pt_{adj} isomer is now dominant in the spectrum and Pt_{rem} has almost disappeared into baseline. * = unidentified

From the ^{1}H NMR data it appears that the initially formed product is not the isomer that theory predicts to be thermodynamically favoured. Instead the energetically less favourable Pt_{rem} forms first and when left in chloroform for a period of time it slowly isomerises to form the Pt_{adj} isomer, shown in Figure 3.9, which is predicted to be lower in energy. Isomerisation of the type shown in Figure 3.10 can be ruled out by the observed platinum coupling on one isomer but not the other.

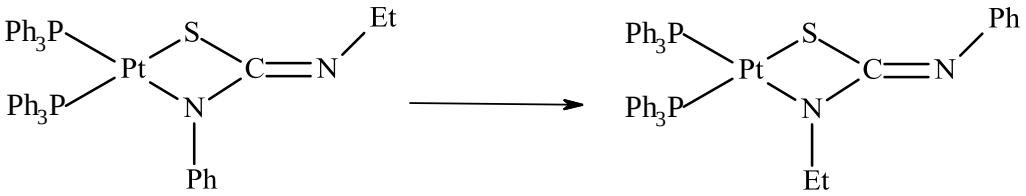

Figure 3.9 Illustration of the structural changes from Pt_{rem} to Pt_{adj}

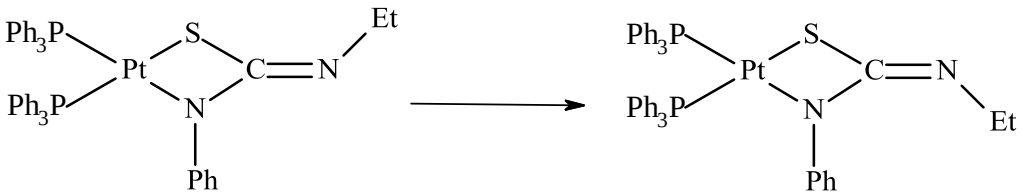

Figure 3.10 Rotation isomerisation of the Et group from 'upward' to 'downward' can be ruled out from the evidence of platinum coupling

To further confirm that the changes were not due to decomposition, ES-MS was obtained on the solid remaining after evaporation of the NMR solvent. This showed a clean spectrum, with the dominant Pt isotope peak for the $[M+H]^{+}$ ion unchanged from the *m/z* value for the first ES-MS.

The isomerism is also clearly evident in the ^{31}P NMR spectra. The expected signal pattern is two doublets each with a set of satellites due to platinum coupling. Two

doublets in an AB pattern each having two much lower intensity satellites equal distance from the main peak, caused by P-Pt coupling. This pattern is congruent with two inequivalent phosphorus atoms.

The isomerisation of the compound from Pt_{rem} to Pt_{adj} causes the AB pattern doublets to shift. The Pt_{rem} isomers main signals have chemical shifts of δ 15.9/11.4 ppm, the Pt_{adj} isomers main signals occur at δ 18.7/13.6 ppm. The P-P coupling constant remains 22 Hz and the P-Pt coupling constant remains approximately 3100 Hz. These comparable coupling values confirm that the compound undergoes an isomerisation process, rather than a drastic structural change such as altering the coordination mode. Figure 3.11 shows the ^{31}P NMR spectra of the compound mid-way through the isomerisation process. The AB signals and the satellites are visible for the Pt_{rem} isomer, and the smaller AB signals correspond to the Pt_{adj} isomer, the satellites for this isomer are not yet intense enough to be observed above the baseline.

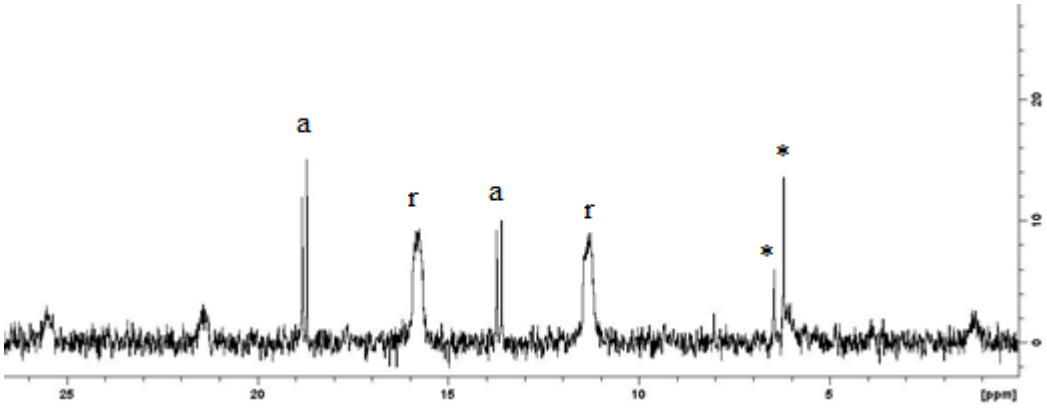

Figure 3.11 ^{31}P NMR spectrum of L_{PhEt} showing the two AB pattern signals concurrent with the compound mid isomerisation, a and r on the spectrum indicate the peaks corresponding to Pt_{adj} and Pt_{rem} respectively. * = unidentified

3.1.2 Investigating possible causes of isomerisation

Isomerisation in the solution phase is not a novel concept; many other unrelated compounds undergo the same process. [29,30] However, there is no literature specific to thiourea dianion isomers that confirms or explains why this occurs, only a suggestion that two different isomers could form. The structurally similar platinum compound with a semicarbazide ligand does form a mixture of isomers [26] and on the basis of this result the authors postulated that thioureas could also form two isomers. This prediction was entirely reasonable; it was thought that the thiourea compounds would form mixtures of the two possible isomers, with the ratio dependant on the energy barrier between the two structures. There was no evidence reported to suggest that these compounds would form one structure and then undergo solution phase isomerism to form the other. This discovery was unexpected and posed a number of questions as to why and how the compound was undergoing this process.

A number of experiments were carried in an attempt to eliminate solid state and solvent interactions as major influences on the formation of isomers. These could be easily disproved using spectral and theoretical data.

If solid state interactions were the cause then it would be assumed that the compound would be one isomer in solution and the other isomer as a solid. From the NMR data it appeared that the initially formed precipitate consists of one isomer, and that when it is dissolved it isomerises into the opposite isomer.

If the initial precipitate and the product from the evaporated NMR sample were proved to be the same isomer then a solid state interaction is more likely. To test this, solid state analytical techniques were used. Both the initial precipitate and the solid from the evaporated NMR sample were examined by FTIR and Raman

spectroscopy. The two compounds differed significantly enough in each of these techniques enough to presume that the two solids are in fact the two different isomers. Figure 3.12 shows the Raman spectra for each solid, the area of significant difference is boxed in red on each spectrum.

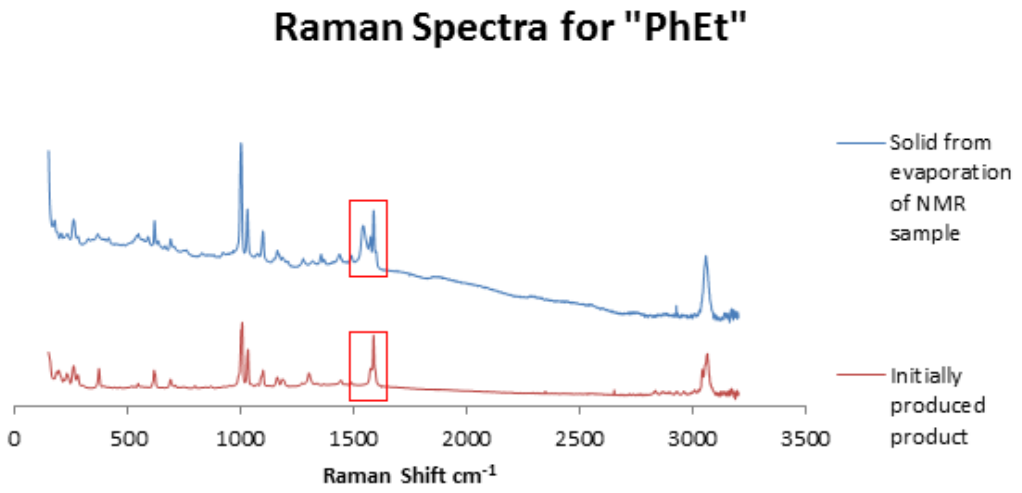

Figure 3.12 Raman spectra for both the initially formed product (Pt_{rem}) and the solid from the evaporated NMR sample (Pt_{adj}) of the compound $(Ph_3P)_2SC(=NEt)NPh$

Further confirmation that isomerism is not caused by solid state interactions was obtained when the solid from the evaporated NMR sample was dissolved in $CDCl_3$ and reanalysed. The ^1H spectrum contains only peaks corresponding to the Pt_{adj} isomer.

Solvent interactions were another possible cause for isomerisation. During its synthesis, the compound encounters methanol and water and deuterated chloroform during NMR analysis. Water was used to precipitate the compound after it was refluxed in methanol, due to the compound being insoluble in water,

and the fact that isomerisation takes place in solution phase, it is unlikely that water is a cause.

Theoretical calculations showed that the energy difference between the two isomers changed by a negligible amount in the solvents used (Table 3.1). GPt_{rem}-GPt_{adj} will result in a positive difference when Pt_{adj} is dominant and negative when Pt_{rem} is dominant. It is also evident from the same table that each compound has the same sign for the difference in each solvent, so the same isomer is predicted to be dominant independent of solvent type. The solvent plays no substantial part in which isomer will form.

Table 3.1 Difference in calculated electronic energies (Pt_{rem}-Pt_{adj}) for $(Ph_3P)_2PtSC(=NR)NPh$ in the different solvents. All values are reported in kJ mol^{-1}

R group	$CDCl_3$	MeOH	H_2O
Me	17.1	16.8	16.6
Et	18.6	18.2	18.0
Pr	20.0	18.6	18.4
Pr^i	9.1	7.1	6.8
Bu^n	21.7	20.7	20.4
Bu^t	-19.5	-19.6	-19.7
p-tol	2.0	1.7	2.9

Thermodynamic and kinetic favoured products appear to be the cause of the isomerisation process observed. It is suggested that Pt_{rem} is the kinetically stable product and Pt_{rem} forms during the synthesis (reflux). When the cold distilled water is added Pt_{rem} precipitates as a yellow solid. When the initial precipitate is dissolved in $CDCl_3$ for NMR analysis the kinetically favoured isomer slowly isomerises into the thermodynamically favoured product, Pt_{adj}, and remains as this

isomer when the solvent is evaporated. It is possible that if the reflux mixture is left to cool to room temperature before the water is added, then the compound will have time to resolve into the thermodynamically favoured isomer in solution. To test this hypothesis a new batch of the compound was made. After refluxing, some of the hot solution was removed and cold water added to it immediately. The remainder was left for 3 days in the reaction flask and then cold water added. The two resulting solids had distinctly different colours. When NMR analysis was carried out the immediately precipitated solid showed the same isomerisation process as previous batches of this compound, changing from Pt_{rem} into Pt_{adj} in solution. The compound precipitated after 3 days did not undergo any chemical shift changes and contained only the lower energy Pt_{adj} structure.

From the NMR study it appears that the isomerisation can be attributed to formation of a kinetically favoured product, and that the change will only occur in solution phase.

3.1.3 X-Ray crystal structure of $(Ph_3P)_2PtSC(=NPh)NEt$

X-ray quality crystals were produced by room temperature vapour diffusion using dichloromethane and pentane solvents. The complete structure was unrefinable due to areas of undetermined electron density, largely involving incorporated solvent molecules. The connectivity of the metal complex however is undisputable and is the Pt_{adj} isomer, Figure 3.13.

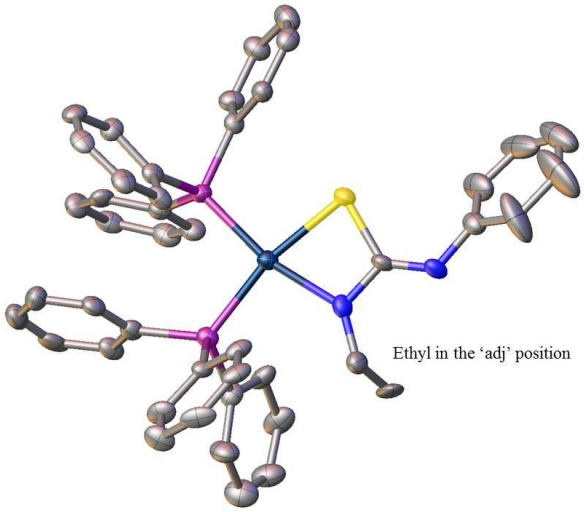

Figure 3.13 X-ray crystal structure of L_{PhEt}, showing the connectivity to be that of the Pt_{adj} isomer

3.2 Platinum complexes containing other n-alkyl substituted thiourea dianion ligands

The other n-alkyl substituted thiourea dianion ligands are predicted to behave in the same manner as L_{PhEt} due to the structural similarities. Theoretical calculations showed the energy differences between the isomers of L_{PhMe}, L_{PhPrn} and $_{LPhBun}$ to be of the same sign and similar magnitudes to the L_{PhEt} compound (Table 3.2). The comparability of these values lead to the expectation that the Pt_{adj} isomer will be the thermodynamically favoured form.

Table 3.2 Difference in Gibbs free energy between Pt_{adj} and Pt_{rem} isomers [$\Delta G(GPt_{rem}\text{-}GPt_{adj})$] in the gas phase

R	ΔG kJ mol^{-1}
Me	31.7
Et	20.8
Pr^n	22.8
Bu^n	23.4

From studies performed on the L_{PhEt} compound it was established that the isomers are not in thermal equilibrium when first made. The kinetically favoured isomer, Pt_{rem}, is formed initially and when dissolved, slowly transforms into the thermodynamically favourable isomer Pt_{adj}. This evidence of kinetic products forming renders the Boltzmann distribution, and any predictions about population of states made with it unreliable. Due to the structural similarities between L_{PhEt} and this group of n-alkyl substituted compounds and the comparable sign and magnitude of their $\Delta G(GPt_{rem}\text{-}GPt_{adj})$ values, it was predicted that they would undergo the same isomerisation process.

The same NMR studies that were done on the L_{PhEt} compound were repeated on these compounds. These studies proved that they do form the Pt_{rem} isomer initially, then isomerise into the more favourable Pt_{adj} in solution. The longer the alkyl group, the less distinctly the isomerisation is visible in the ^{1}H spectra, due to the overlapping multiplets on the spectra that correspond to the central CH_2 groups of a long chain alkyl. In particular in the L_{PhBun} compound the multiplets corresponding to the central CH_2 groups do not resolve, and the sets from each isomer overlap. The triplet signal appears as an unresolved singlet in the Pt_{adj} isomer signal, but when integrated appears to have equal contributions as the Pt_{rem} triplet. A comparison of the complex before and after isomerisation is shown in Figure 3.14.

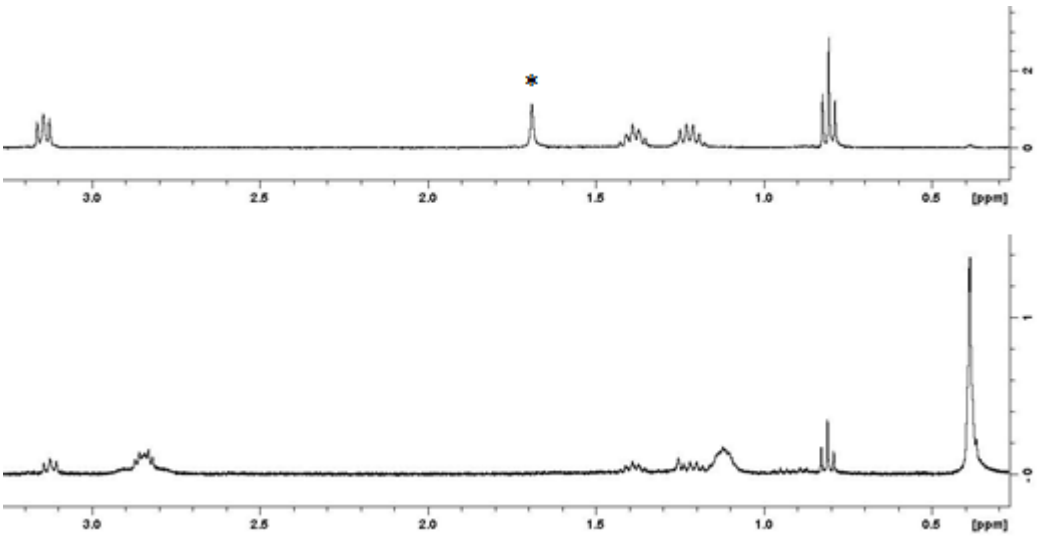

Figure 3.14 ^{1}H spectra of the L_{PhBun} compound before and after isomerisation. * = unidentified

The ^{31}P NMR signals show a relationship between the chemical shift of the major AB doublet signals and the kinetically or thermodynamically favoured isomer. Table 3.3 shows that the thermodynamically favoured isomer has signals at approximately δ 18/14 ppm and the kinetically favoured isomers signals are more upfield at approximately δ 16/12 ppm, regardless of which compound is being investigated. In each of these n-alkyl substituted complexes the Pt_{adj} isomer is dominant and is downfield of the Pt_{rem} isomer. ^{31}P chemical shifts are very sensitive to environment [31] so the Pt_{adj} and Pt_{rem} isomers can be distinguished based on their chemical shift.

Table 3.3 ^{31}P NMR chemical shift values for the major AB doublet signals attributed to both Pt_{rem} and Pt_{adj} in $CDCl_3$

	Chemical Shift (ppm)			
R	A_{rem}	B_{rem}	A_{adj}	B_{adj}
Me	16	11.5	18	13.9
Et	15.9	11.4	18.7	13.6
Pr^n	16.9	12.2	19	13.7
Bu^n	16.5	11.9	18.9	13.7

There is also an apparent trend between the rate of isomerisation and the energy difference of the two isomers. L_{PhMe} has the highest $\Delta G(GPt_{rem}\text{-}GPt_{adj})$ value, and after 30 min in solution the Pt_{rem} isomer has almost completely isomerised into Pt_{adj}. The compounds L_{PhEt}, L_{PhPrn} and L_{PhBun} have very similar $\Delta G(GPt_{rem}\text{-}GPt_{adj})$ values, all within 2 kJ mol^{-1} and they each have a comparable isomerisation time of approximately 90 min, which is 60 minutes more than the time taken for L_{PhMe} to isomerise.

Each of these compounds only increases the size of the R group away from the platinum coordination site. The increase in length of the substituent does not appear to have a significant effect on the difference in energy between the two isomers, beyond the first carbon. The decrease in $\Delta G(GPt_{rem}\text{-}GPt_{adj})$ magnitude from Me to Et is significant, 10 kJ mol^{-1}, but with the addition of a third and fourth carbon the energy difference does not alter significantly.

3.3 Conclusions drawn from the n-alkyl substituted thiourea dianion complexes

Beyond two carbons, increasing the length of the alkyl chain has minimal impact on the energy difference between the two isomers. Figure 3.15 illustrates graphically the large drop when the second CH_3 is added to the chain (Me-Et) and the considerably smaller increases as the third and fourth CH_3 groups are added (Et-Pr^n-Bu^n).

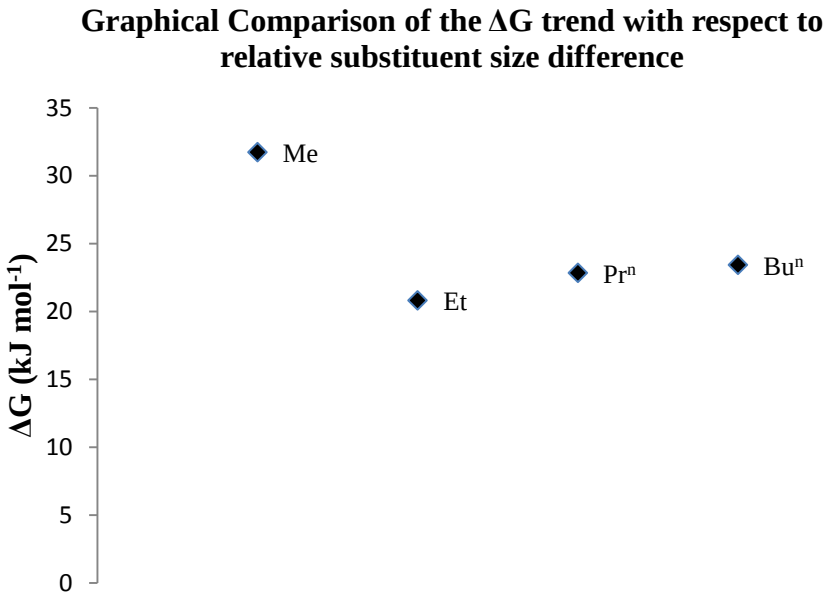

Figure 3.15 Graph illustrating the ΔG trend as the length of the straight chain alkyl group increases

This data lead to the conclusion that 'bulk' directly attached to the nitrogen adjacent carbon will have the greatest effect on $\Delta G(GPt_{rem}\text{-}GPt_{adj})$. To investigate this theory the branched alkyl substituted thiourea dianion complexes L_{PhPri} and L_{PhBut} were synthesised. The aromatic substituted compound $L_{Ph\textit{p}\text{-tol}}$ was also synthesised as it was assumed that the energy barrier between the two isomers would be very low due to the structural similarities of Ph and *p*-tol.

Chapter 4 Platinum complexes containing branched alkyl and aromatic substituted thiourea dianion ligands

This chapter contains results and discussion of theoretical and spectral data for the platinum compounds containing thiourea dianion ligands substituted with branched alkyl and aromatic groups. These compounds were synthesised to investigate the trends postulated after the investigation of the n-alkyl substituted thiourea dianion complexes. The branched alkyl and aromatic compounds are discussed in sets related to substituent type, as their results have differences too significant to discuss as groups. Trends determined from the results are collected into a section at the end of this chapter.

4.1 $(Ph_3P)_2PtSC(=NPr^i)NPh$ (L_{PhPri})

L_{PhPri} has the same sign for $\Delta G(GPt_{rem}\text{-}GPt_{adj})$ as the n-alkyl substituted compounds but only half the magnitude, $\Delta G(Pr^i)$ = 11.1 kJ mol^{-1}. This significantly smaller energy difference was expected to impact on the rate of isomerisation, but not the direction. The Pt_{adj} isomer was still predicted to be thermodynamically favourable. The n-alkyl compounds all show isomerisation indicators within minutes of dissolution, and the process is completed after 2-3 hours. L_{PhPri} had a much slower rate which fitted well into the assumed relationship between $\Delta G(GPt_{rem}\text{-}GPt_{adj})$ and isomerisation rate partly established by the n-alkyl thioureas.

Unlike the n-alkyl compounds which show the isomerisation process distinctly in the ^1H spectra, the proton spectrum for the assignment of L_{PhPri} is more complicated. The Pt_{adj} isomer is usually identified by $^3J_{Pt\text{-}H}$ coupling. L_{PhPri} has the

potential to have platinum coupling, but the six protons on the adjacent carbons mean that it was unresolved on the sides of the multiplet which will be present in both the Pt_{adj} and Pt_{rem} isomers. Although small chemical shift changes in the ^{1}H spectrum were observed over time the isomerisation is more easily detected and the signals assigned to isomers in the ^{31}P NMR spectra.

Figure 4.1 shows the ^{31}P NMR spectrum 30 minutes after the dissolution of the solid sample in $CDCl_3$. This spectrum showed no evidence of a second isomer with different chemical shifts. After 2.5 hours, Figure 4.2, doublets appear at 20/14 ppm, the first sign that L_{PhPri} is isomerising. After 26 hours, Figure 4.3, the same sample was analysed again by ^{31}P NMR and in the resulting spectrum the AB signals had changed chemical shift to a more downfield position. L_{PhPri} has a much slower rate of isomerisation. The energy difference between the two structures is not small enough to allow a mixture of isomers to form, but not high enough that the compound begins to isomerise immediately. This observation reinforces the correlation between substituent size difference, $\Delta G(GPt_{rem}\text{-}GPt_{adj})$ and isomerisation rate. As the R groups steric size becomes similar to the Ph groups steric size, the rate of isomerisation decreases. The smaller the energy differences between the two isomers, the slower the rate of isomerisation. From this trend it could be predicted that a substituent close in size to Ph, which will have a low energy difference, would not isomerise at all or form a stable mixture of the two structures.

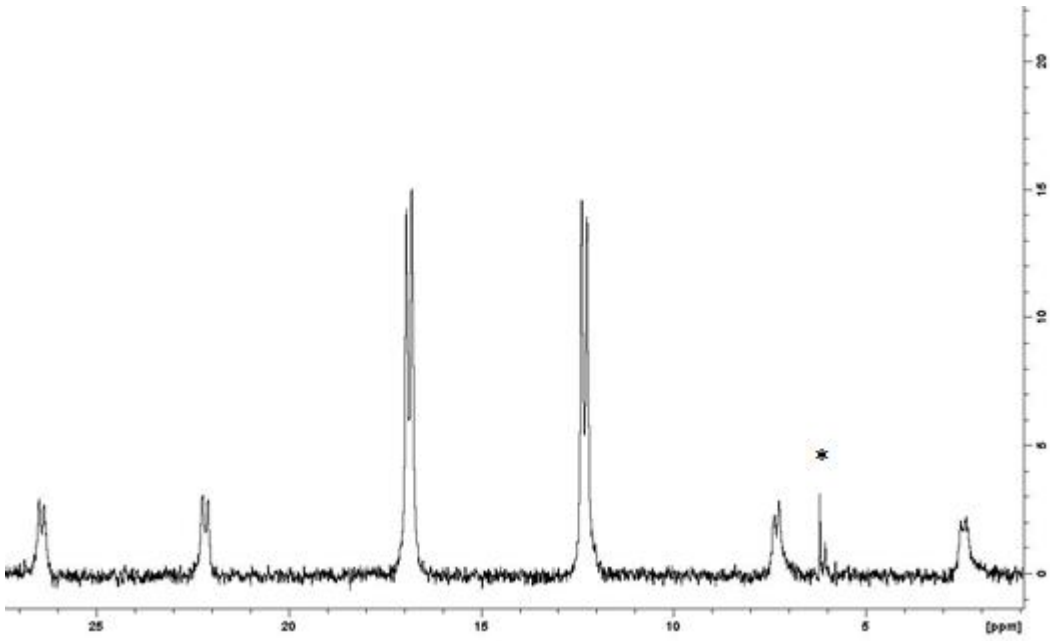

Figure 4.1 ^{31}P NMR spectrum of L_{PhPri} in $CDCl_3$ after 30 minutes in solution, no second isomer visible. * = unidentified

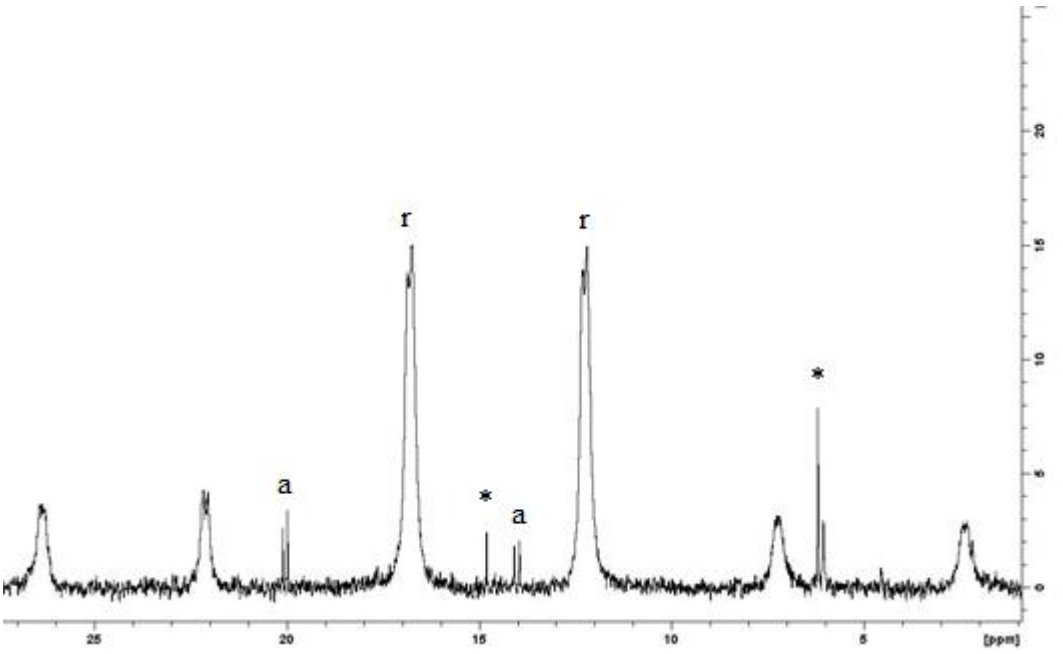

Figure 4.2 ^{31}P NMR spectrum of L_{PhPri} in $CDCl_3$ after 2.5 hours, the second isomer (adjacent, a) is just beginning to appear over the baseline. * = unidentified

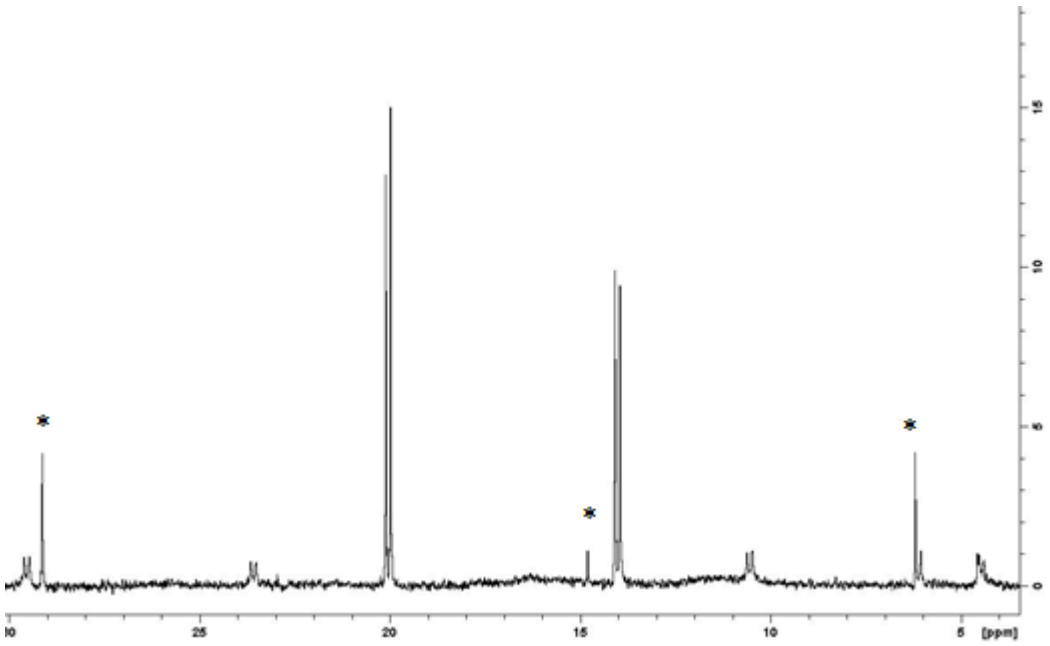

Figure 4.3 ^{31}P NMR of L_{PhPri} after 26 hours, the first isomer has now disappeared and only the Pt_{adj} isomer is present. * = unidentified

The thermodynamically favoured isomer was identified as Pt_{adj}, based on the sign of $\Delta G(GPt_{rem}\text{-}GPt_{adj})$, the chemical shifts of the ^{31}P signals and platinum coupling observed in the ^{1}H NMR.

The n-alkyl compounds identified a trend in the chemical shift of each isomer's ^{31}P signals. The Pt_{adj} isomer is consistently more downfield at δ 18/13 ppm than the Pt_{rem} isomer is at δ 16/12 ppm. The L_{PhPri} has shifted the whole spectrum downfield when compared with the n-alkyl compounds δ 20/14 ppm for Pt_{adj} and Pt_{rem} δ 17/12 ppm; however, the Pt_{adj} isomer is still more downfield than the Pt_{rem} so the trend is still valid. The thiourea dianion complexes substituted with Me, Et, Pr^{n} and Pr^{i} groups show the Pt_{adj} isomer to be more downfield than the Pt_{rem} isomer in their ^{31}P NMR spectra. It is not yet possible to assume that the Pt_{adj} will always be more downfield, regardless of whether it is thermodynamically favoured or not.

4.2 $(Ph_3P)_2PtSC(=NBu^t)NPh$ (L_{PhBut})

The tertiary butyl group has a very large steric bulk. If the conclusions drawn from the n-alkyl substituted thiourea dianion complexes (3.3) are correct then this will result in a large energy difference between the Pt_{adj} and Pt_{rem} isomers. Theory calculates the $\Delta G(GPt_{rem}\text{-}GPt_{adj})$ value to be -31 kJ mol^{-1}, which predicts Pt_{rem} to be the thermodynamically favoured isomer. This prediction is opposite to that of the straight chain alkyls, but not unexpected due to the large steric bulk of the Bu^t group. Figure 4.4 shows a space filling view of the crystal structure of the L_{PhPh} compound reported by Henderson *et al*. In this image the phenyl group adjacent to the platinum is visibly restricted in its orientation by the triphenylphosphine groups surrounding it. The phenyl group must rotate sideways to slot into the relatively small space between the PPh_3 groups of adjacent molecules. The three dimensional nature of a Bu^t group means it does not have a 'flat' orientation.

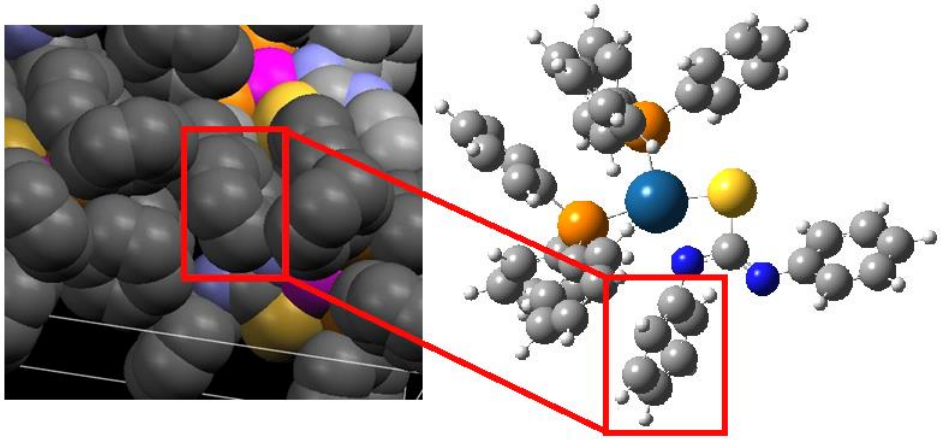

Figure 4.4 Spacefilling view of the crystal structure of L_{PhPh}, illustrating the limited space available in the Pt_{adj} position

When ^1H NMR studies were carried out on L_{PhBut} there was evidence of isomerisation occurring. Although the change in chemical shift is not as

distinctive as the other compounds the 0.01 ppm shift for the Bu^t group is notable by the dramatic switch in intensity, Figure 4.5.

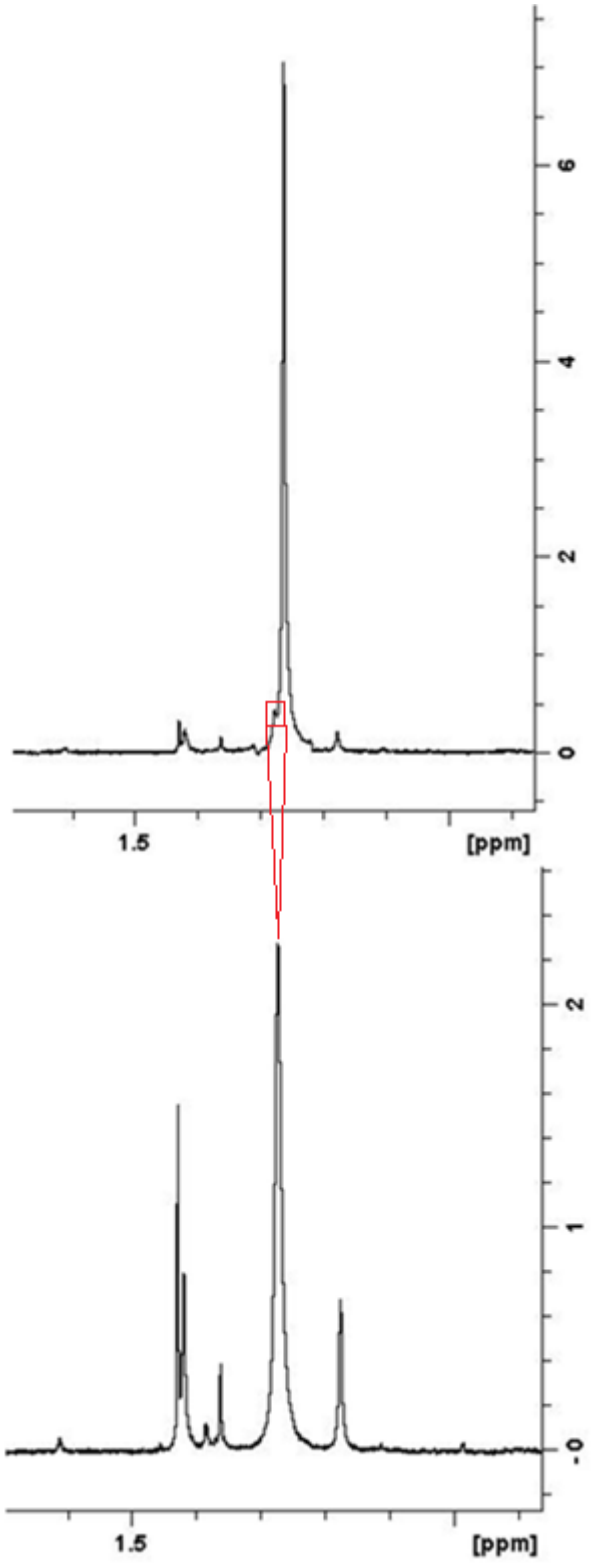

Figure 4.5 ^{1}H spectra of $(Ph_3P)_2PtSC(=NBu^t)NPh$ before (top) and after (bottom) isomerisation

The ^{31}P NMR spectra show the isomerisation more distinctly. The spectrum after two hours in solution, Figure 4.6, has two sets of AB pattern signals, and their accompanying platinum satellites, indicating that two isomers are present. After 26 hours in solution the spectrum only has one AB signal pattern, which indicates that only one isomer is now present, Figure 4.7.

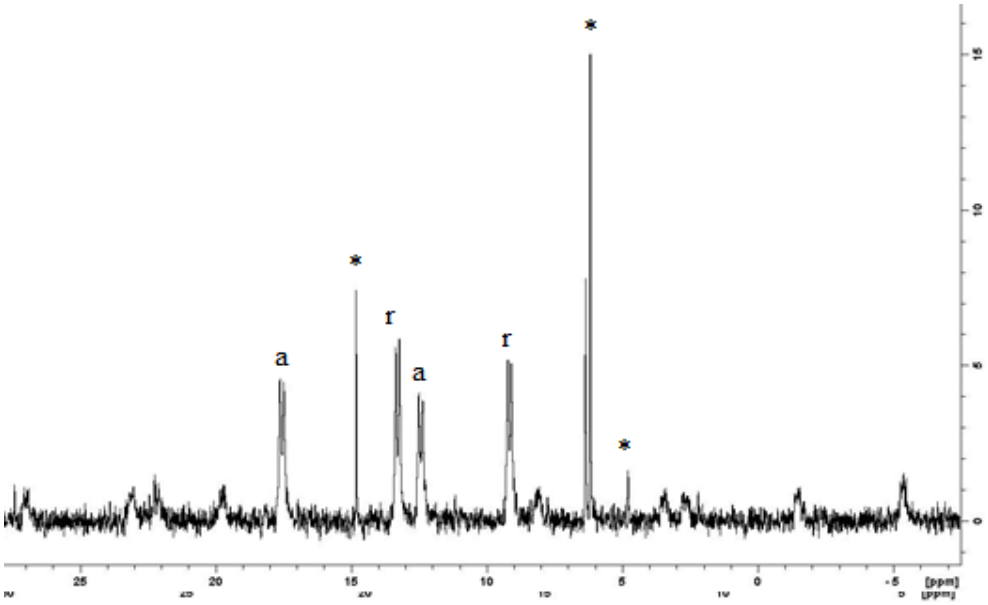

Figure 4.6 ^{31}P NMR spectrum showing of $(Ph_3P)_2PtSC(=NBu^t)NPh$ two AB pattern signals, indicating the presence of two isomers. * = unidentified

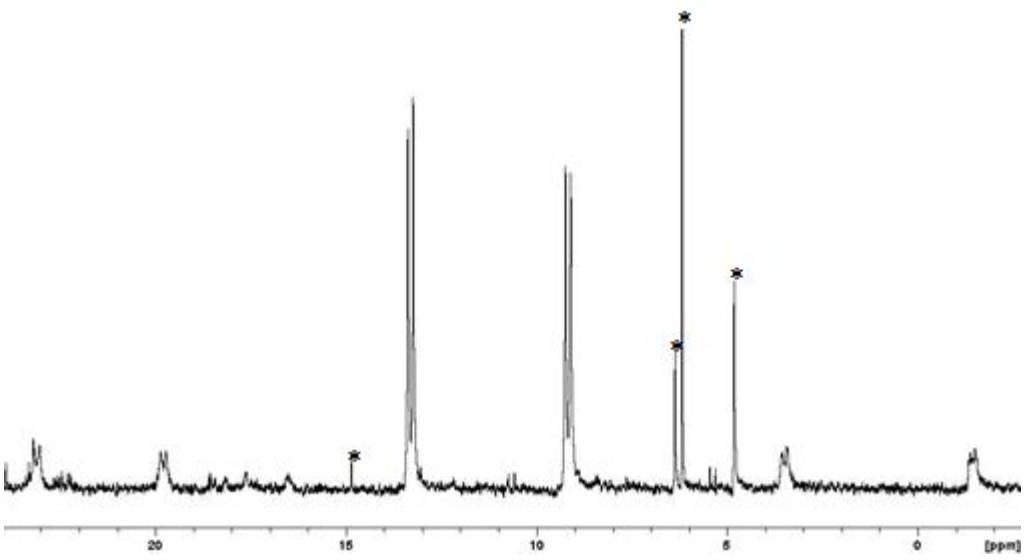

Figure 4.7 ^{31}P NMR spectrum of $(Ph_3P)_2PtSC(=NBu^t)NPh$ showing only one isomer. * = unidentified

Previously, the two isomers have been differentiated from one another by the presence of $^{3}J_{Pt\text{-}H}$ coupling on the ^{1}H signal of the alkyl substituent corresponding to the Pt_{adj} isomer. Due to the structure of Bu^{t} no Pt-H coupling can be observed. Spectral evidence to support the assignment of each isomer is lacking, but assumptions can be made by comparing theoretical calculations to ^{31}P chemical shifts. The isomer formed after isomerisation could have been unquestionably determined by the use of X-ray crystallography, however, attempts to crystallise this compound were unsuccessful.

Theory correctly predicted the thermodynamically favourable isomer for the n-alkyl substituted compounds, so the assumption was made that theory will correctly predict the thermodynamically favourable isomer for the non n-alkyl compounds too. In the case of L_{PhBut} the Pt_{rem} isomer is calculated to be 31 kJ mol^{-1} lower in energy than the Pt_{adj} isomer.

The major ^{31}P signals calculated for each isomer from DFT were matched to each set observed experimentally, allowing each pair of AB signals to be assigned to either Pt_{adj} or Pt_{rem}. Theoretical NMR calculations do not show any coupling, so the Pt satellites are not visible and each peak appears as a singlet not a doublet as they are experimentally. Each of the AB signals has a distinctly different distance between the A and the B doublet. The relative distance between the two experimental peaks can be matched to the relative distance between the theoretical peaks. The Pt_{rem} isomer has a calculated A-B separation of 21.5 ppm, Ptadj has a calculated A-B separation of 27.6 ppm. These values can be matched to the two experimentally observed AB signals. The signal with the smaller A-B distance corresponds to the Pt_{rem} isomer (r in Figure 4.6, A-B = 4.1 ppm) and the AB signal

with the larger A-B distance corresponds to Pt_{adj} (a in Figure 4.6, A-B = 5.2 ppm). Figure 4.7 shows the ^{31}P NMR spectrum of L_{PhBut} after the isomerisation process is complete. The signals at δ 13/9 ppm remain; these are the more upfield signals, which have been assigned to the Pt_{rem} isomer based on theoretical energy and NMR calculations. In Section 3.2, it was postulated that the Pt_{adj} isomer will always have chemical shift values more downfield than the Pt_{rem} isomer, regardless of its stability. The L_{PhBut} complex isomerises from Pt_{adj} into Pt_{rem}, however, the Ptadj ^{31}P NMR signals are still of comparable chemical shift to the Pt_{adj} ^{31}P NMR signals of the other asymmetric thiourea dianion complexes.

4.2.1 Conclusions drawn from the branched alkyl substituted thiourea dianion complexes

The branched alkyl series of Me, Et, Pr^i and Bu^t show a relationship between the number of CH_3 groups on the nitrogen adjacent carbon (Figure 4.8). The idea that $\Delta G(GPt_{rem}\text{-}GPt_{adj})$ is most greatly influenced by adding bulk to this area was postulated after it became evident that increasing the alkyl chain length has minimal effect on $\Delta G(GPt_{rem}\text{-}GPt_{adj})$ (Section 3.3).

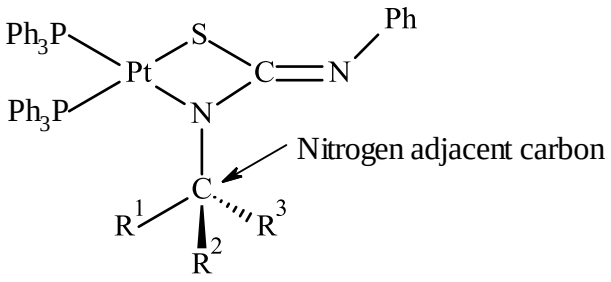

Figure 4.8 Illustration of the nitrogen adjacent carbon

Figure 4.9 shows the trend in ΔG for the branched alkyl series. It is clear that the addition of each methyl group onto the nitrogen adjacent carbon has a large impact on the energy difference between the Pt_{rem} and Pt_{adj} isomers. L_{PhMe}, L_{PhEt}

and L_{PhPri} all favour the Pt_{adj} isomer, while L_{PhBut} favours the Pt_{rem} isomer. The dramatic drop in energy from the L_{PhPri} complex to the L_{PhBut} complex can be attributed to substituent shape. The Me, Et and Pr^i groups all have at least one hydrogen on the nitrogen adjacent carbon, which is orientated towards the bulky PPh_3 groups to minimise the space used. The Bu^t group does not have a hydrogen to orientate in this way to minimise the steric bulk effect, instead it must direct a considerably bulkier methyl group in this direction, shown in Figure 4.10, the optimised structures of L_{PhPri} and L_{PhBut}.

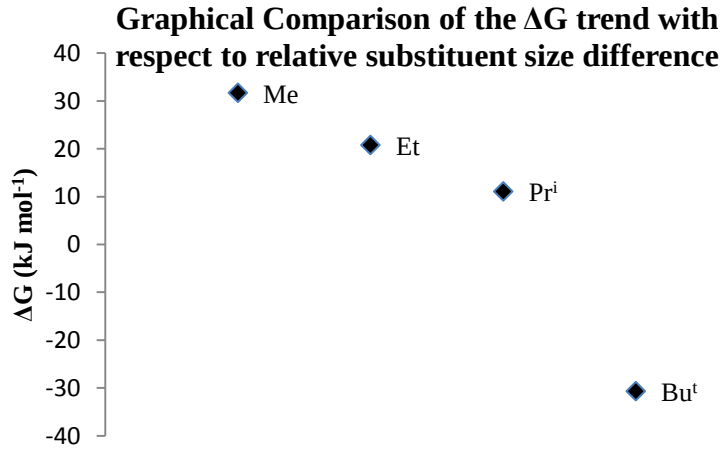

Figure 4.9 Graph illustrating the decreasing ΔG trend as the number of CH_3 groups on the nitrogen adjacent carbon increases

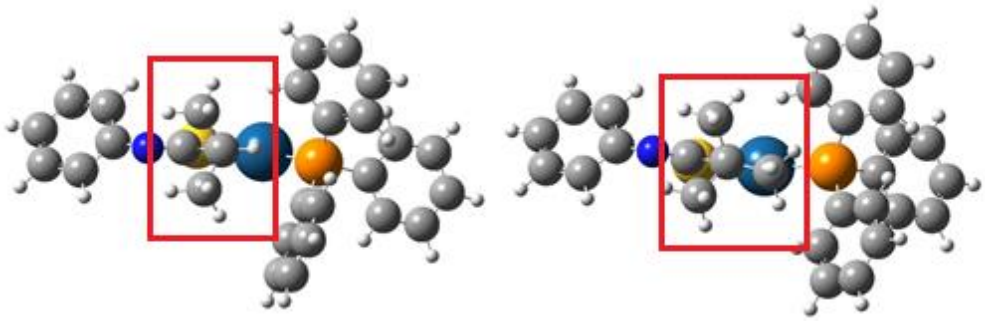

Figure 4.10 DFT optimised structures of L_{PhPri} and L_{PhBut} respectively, looking down the C-N bond, showing the orientation of the H and CH_3 groups into the PPh_3 group. Far side PPh_3 group removed for clarity

4.3 $(Ph_3P)_2PtSC(=N$*p*-tol)NPh (L_{Ph*p*-tol}$)

P-toluene/phenyl substitution was selected because it provides almost identical steric influences, while still maintaining asymmetric substitution of the thiourea ligand. This enables the lowest energy difference between the two isomers to be achieved. The Gibbs free energy difference between the two structures is 2.5 kJ mol^{-1}, which is at least four times smaller than the difference between any of the other compound's isomers. L_{Phptol} precipitates as a mixture of both Pt_{adj} and Pt_{rem} isomers, and no net change in proportion is seen over time in either the ^{31}P or ^{1}H NMR spectra when dissolved in $CDCl_3$.

The difference in size between the Ph and *p*-tol substituents is small, shown in Figure 4.11, the only addition being a methyl group. Section 3.2 it was shown that the addition of steric bulk around the carbon group adjacent to the nitrogen directly bonded to the platinum that has the greatest influence on the stability of each isomer. As a direct continuation of this theme it can be assumed that the *para* methyl group is too far removed from the Pt coordination site and will not have any significant influence on the stability of each isomer. The following spectral evidence that this compound forms two isomers and does not undergo net solution phase isomerism reinforces the prediction made in Section 4.1 that the net isomerisation rate would tend toward zero as the substituents get closer together in size.

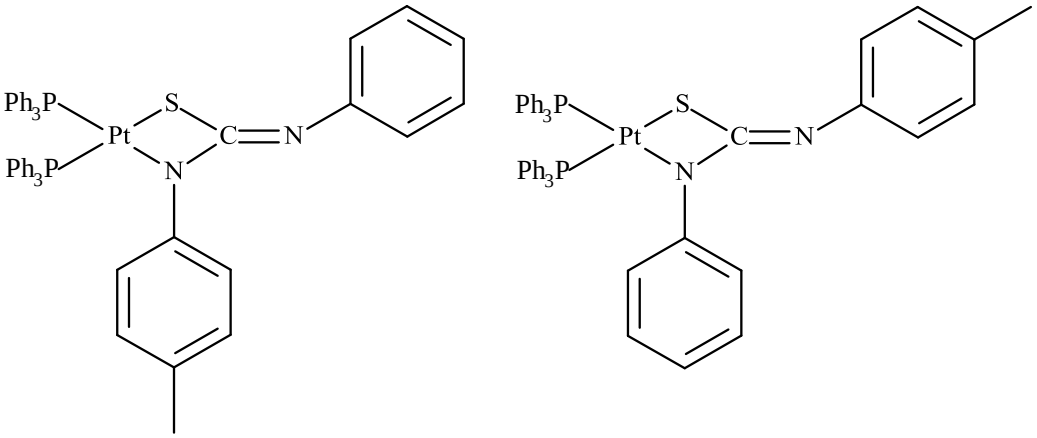

Figure 4.11 Structural illustration of the similarity in size between the Ph and *p*-tol substituents

The ^{1}H NMR spectrum (Figure 4.12, expansion of alkyl region Figure 4.13) of this compound shows the methyl groups on the *p*-tol substituent clearly at 2.18 ppm and 1.96 ppm, in approximately equal proportions. However, which signal corresponds to which isomer was unable to be determined even with the use of 2D NMR techniques. Theory can be used to assist in the assignment of the signals to each isomer. Theoretical NMR calculations predict the chemical shifts of the alkyl region protons to be δ 1.91 ppm for the Pt_{rem} isomer and δ 2.18 ppm for the Pt_{adj} isomer. These are easily matched to the experimental shifts as shown in Figure 4.13.

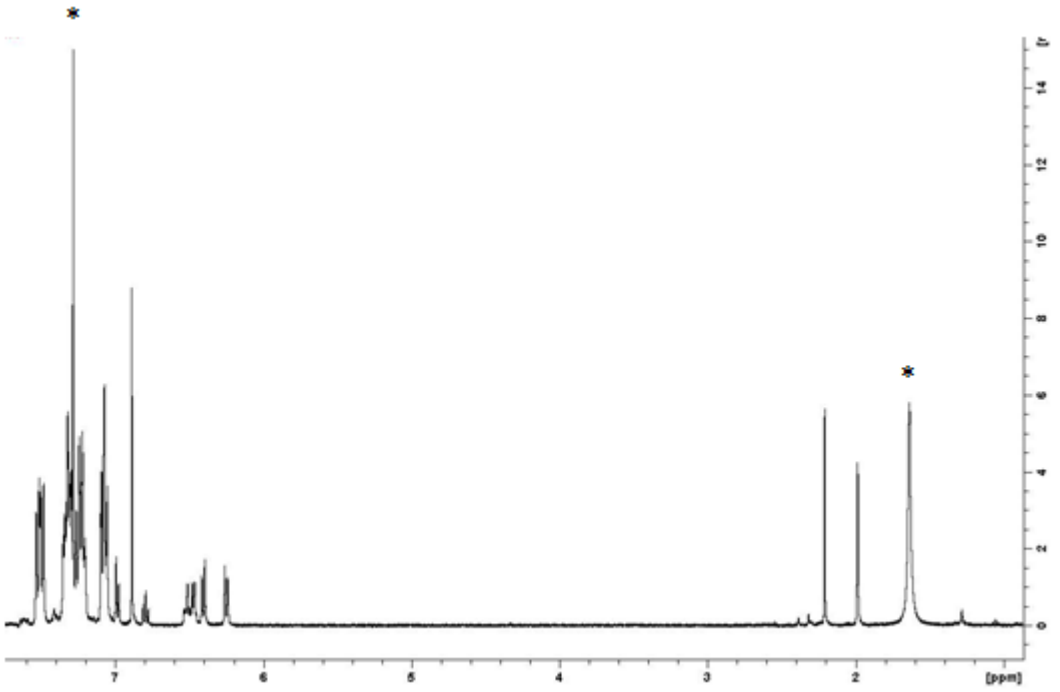

Figure 4.12 ^{1}H spectrum of $L_{Php\text{-}tol}$, * indicates $CDCl_3$ and H_2O respectively.

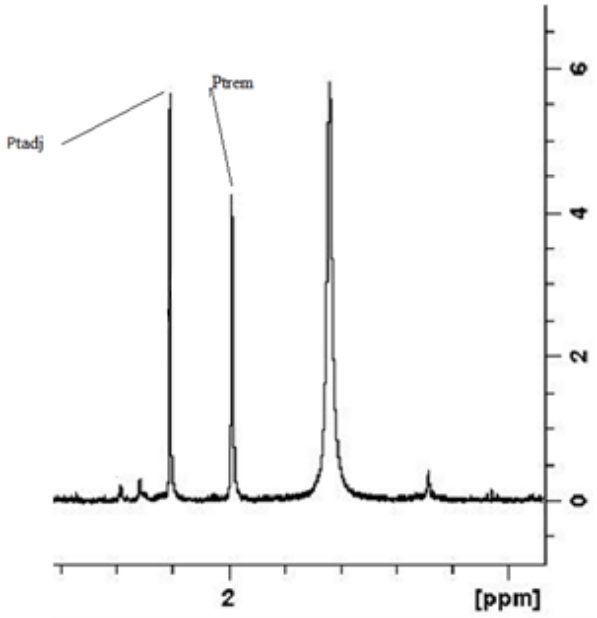

Figure 4.13 Expansion of the alkyl region showing assignments of signals to isomers via the use of theoretical calculations

The ^{31}P NMR spectrum of this same compound shows that the chemical shifts of each isomer are almost identical (Figure 4.14). The AB patterns of each isomer are overlapped, as are the platinum satellites, Figure 4.15.

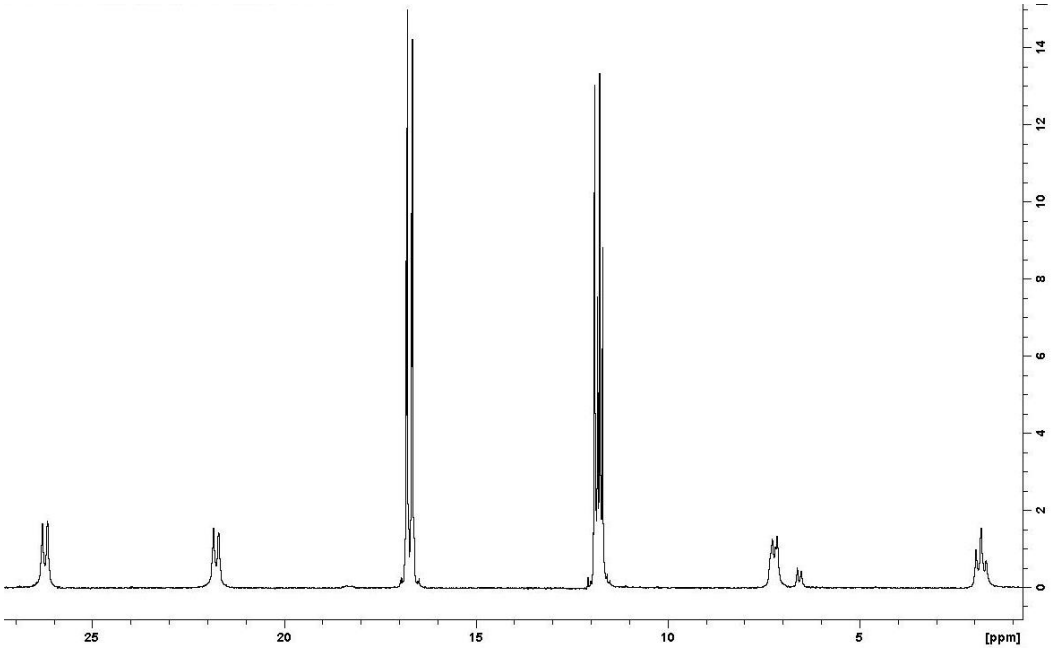

Figure 4.14 ^{31}P NMR spectrum of L_{Phptol} showing overlapping isomer signals

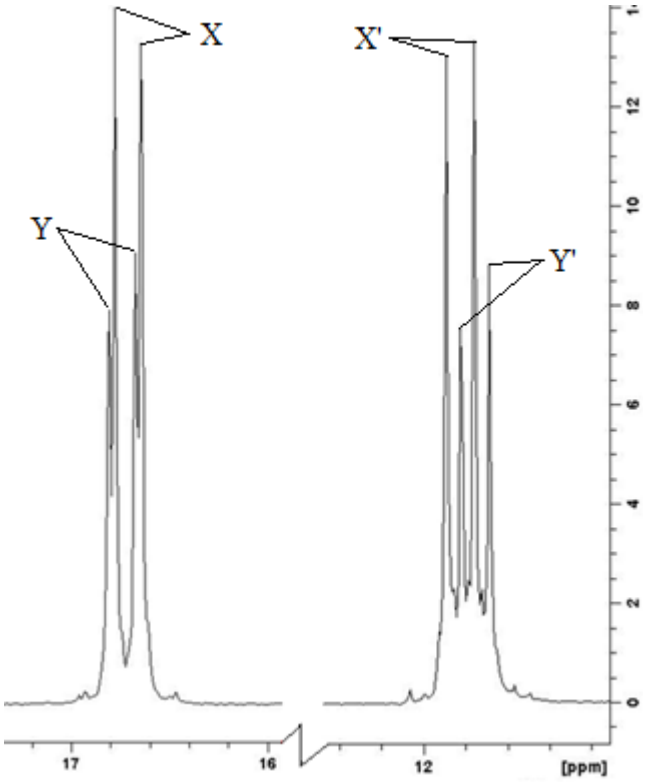

Figure 4.15 Expansion of the ^{31}P NMR spectrum showing the overlapping AB signals for each isomer, X and Y indicate the AB set of each isomer

Chapter 5 Investigation of a platinum complex containing an asymmetrically substituted thiourea monoanion

The monoanion complex $[(Ph_3P)_2SC(=NHEt)NPh]^+$ (L_{PhEtH}) was synthesised. Monoanions with di-phenyl and di-ethyl substituted thioureas have previously been synthesised [13] but a mixed substituent of this kind has not been made with Ph and Et substituents, and those that have been reported have not been the subject of isomerisation studies. When the asymmetric thiourea binds to the platinum as a chelating ligand there are two possible structures that could form. Figure 5.1 illustrates these structures.

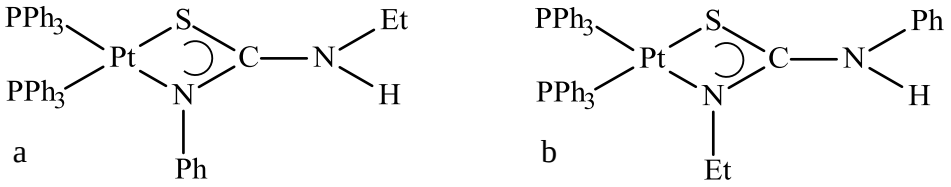

Figure 5.1 The two structures that could be formed when the asymmetric monoanion complex is synthesised.

5.1 Experimental

5.1.1 Synthesis

cis-$PtCl_2(PPh_3)_2$ (309 mg, 0.379 mmol) and PhNHC(S)NHEt (69 mg, 0.384 mmol) were suspended in methanol (20 mL) in a 100 mL round bottom flask with a magnetic stirrer. Et_3N (1.0 mL) was added and the resulting mixture heated to reflux for 5 min. resulting in a clear pale yellow solution. $NaBPh_4$ (134 mg, 0.392

mmol) was added and the suspension cooled on ice for 10 min. The resulting off white precipitate was filtered on a Büchner funnel, washed successively with cold distilled water (5 mL), methanol (5 mL) and diethyl ether (5 mL), and then dried under vacuum.

5.1.2 Characterisation

Melting point: 236-247^{0}C.

ES-MS: Theoretical *m/z* 898.211. The *m/z* for the positive $[M+H]^+$ ion was found to be 898.9966.

FTIR: 3451 (m), 3052 (w), 1643 (w), 1594 (m), 1575 (s), 1480 (m), 1434 (s), 1424 (m), 1397 (w), 1377 (m), 1330 (m), 1312 (w), 1275 (w), 1100 (m), 1091 (m), 1029 (w), 998 (w), 744 (m), 733 (m), 704 (s), 692 (s), 612 (m), 548 (s), 526 (s), 515 (s), 502 (m), 495 (s).

NMR: Pt_{rem}: $^{31}P\{^1H\}$ δ 13.3 ppm [$^1J_{(PtP)}$ 3226 Hz, $^2J_{(PP)}$ 21 Hz] and δ 9.1 ppm [$^1J_{(PtP)}$ 3455 Hz, $^2J_{(PP)}$ 21 Hz], ^1H δ 4.8 [t, N-H, 6 Hz], δ 2.9 ppm [qt, CH_2, $^3J_{(HH)}$ 7 Hz], δ 0.9 ppm [t, CH_3, $^3J_{(HH)}$ 7 Hz]

Pt_{adj}: $^{31}P\{^1H\}$ δ 15.3 ppm [$^1J_{(PtP)}$ 3093 Hz (second satellite unresolved so estimated value), $^2J_{(PP)}$ 21 Hz] and δ 10.1 ppm [$^1J_{(PtP)}$ 2465 Hz, $^2J_{(PP)}$ 22 Hz], ^1H δ 2.3 ppm [q, CH_2, $^3J_{(HH)}$ 7 Hz] and δ 0.8 [t, CH_3, $^3J_{(HH)}$ 7 Hz]

5.2 Results and discussion

The monoanion complex differs from the thiourea dianion complexes in that it does not undergo a net isomerisation process when dissolved. NMR studies do however reveal that the complex does form a stable mixture of two isomers. The ^{31}P NMR spectrum shows a second isomer clearly downfield of the main signals,

at a much lower intensity, Figure 5.2. The second compound visible in this spectrum is assumed to be an isomer of the monoanion complex, the dianion is ruled out due to the chemical shifts of the signals being significantly different. Further proof that the second complex is an isomer is apparent when the spectrum is enlarged, satellite peaks for the low intensity signals appear from the baseline, shown in Figure 5.3, and they have coupling constants within the expected range. It was assumed that the same chemical shift trend that is apparent in the thiourea dianion complexes ^{31}P chemical shift would be apparent in the monoanion. This implies that the Pt_{adj} isomer would still be the more downfield signal. This trend however cannot be blindly applied to the monoanion, and more evidence is required. The two structures can be clearly identified by examining the multiplicity of the ^{1}H NMR signals.

The signals labelled ‘r’ in Figure 5.4 correspond to the isomer shows in Figure 5.1a The CH_2 group of the ethyl compound will couple to both the CH_3 protons and the N-H proton, appearing as a quintet δ 2.9 ppm, the CH_3 will appear as a triplet, δ 0.9 ppm, and the lone proton will appear as a triplet shifted downfield due to the high electronegativity of the nitrogen, δ 4.8 ppm. When the ethyl group is in the adjacent position (Pt_{adj}) Figure 5.1b the CH_2 signal will appear as a quartet, δ 2.3 ppm, and the CH_3 as a triplet, δ 0.8 ppm, these signals are labelled ‘a’ in Figure 5.4.

The relative intensity of the quintet to the quartet proves that the isomer with the Et group in the remote position (Pt_{rem}) is present in much higher concentration than the isomer with the Et group in the adjacent position (Pt_{adj}). It is known that in the equivalent thiourea dianion, L_{PhEt}, the Pt_{adj} isomer is thermodynamically favourable; although Pt_{rem} precipitates initially as a kinetic product and undergoes

a solution phase isomerisation process from Pt_{rem} into Pt_{adj} when dissolved in $CDCl_3$. Due to the structural similarities between the mono and dianion it is expected that the Pt_{adj} would be thermodynamically favoured in both complexes. Evidence that the monoanion Pt_{rem} isomer is dominant in the ^1H NMR spectrum suggests that the extra proton in the monoanion has an inhibiting effect on the mechanism by which the isomerism takes place. It also suggests that the kinetic product formed initially by the thiourea dianion complexes is mechanistically favoured. The protonated monoanion complex is a 'trapped' intermediate.

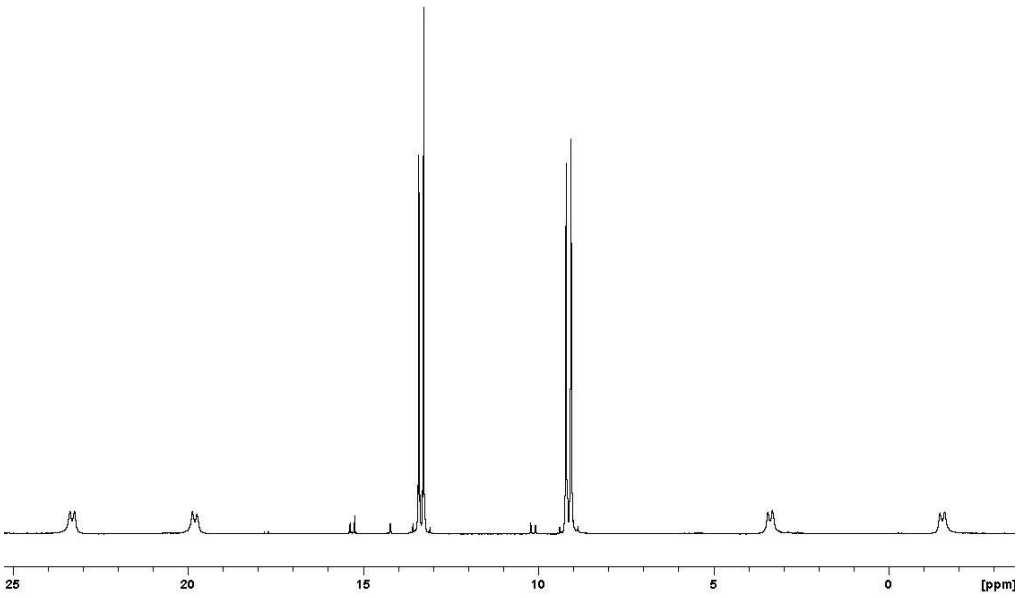

Figure 5.2 The ^{31}P NMR spectrum of the monoanion, second AB signals clearly visible downfield of the main AB signals

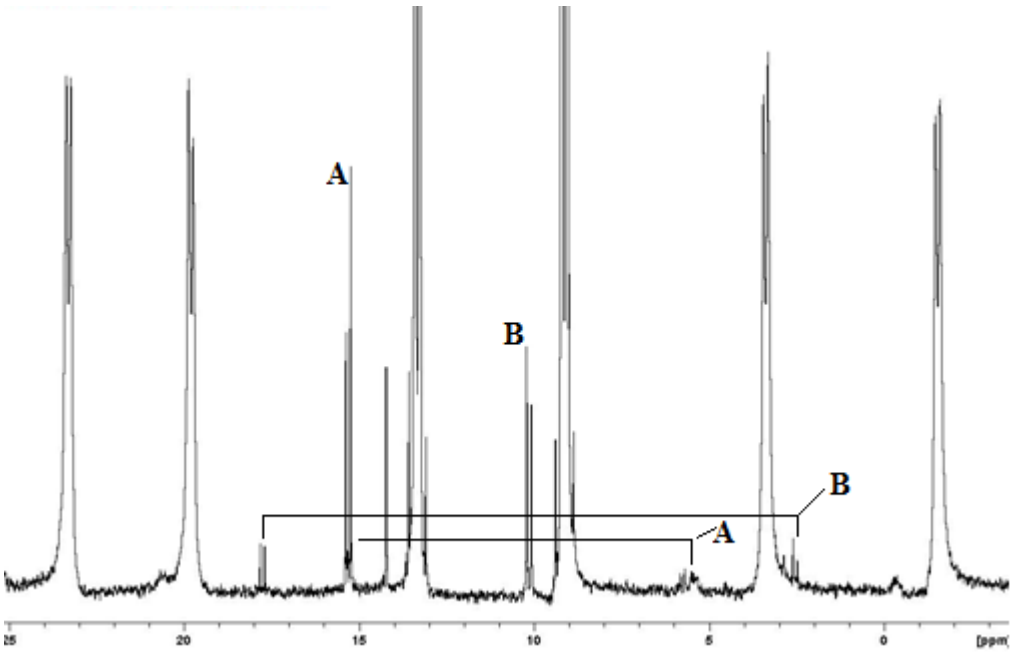

Figure 5.3 Expansion of the ^{31}P NMR spectrum of $[(Ph_3P)_2SC(=NHEt)NPh]^+$ to visualise the minor isomer satellites

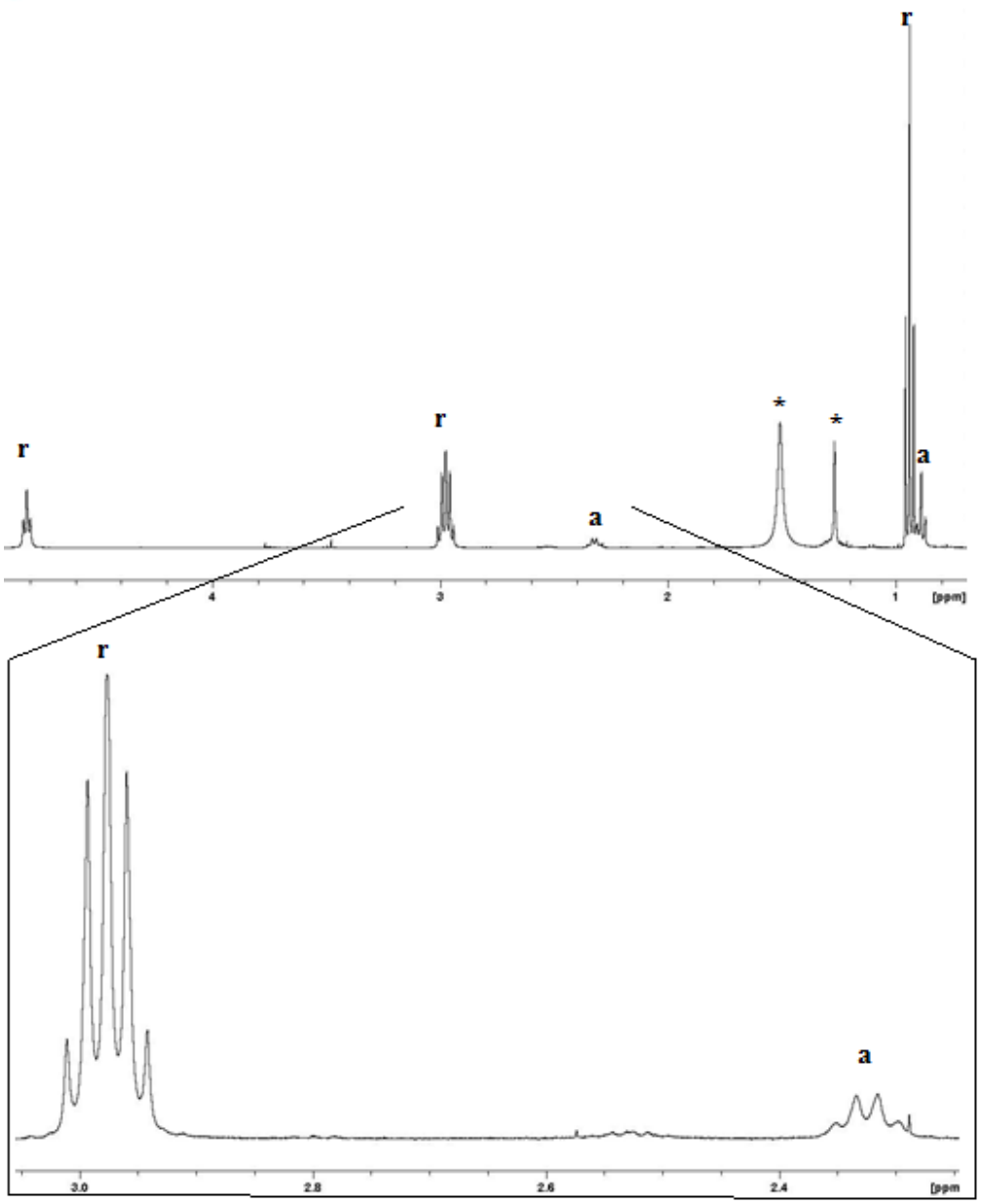

Figure 5.4 Aryl section of the ^{1}H NMR spectrum of the thiourea monoanion complex, $[(Ph_3P)_2SC(=NHEt)NPh]^+$, and an expansion of the quintet and quartet

Chapter 6 Conclusions

Platinum compounds that contain asymmetrically substituted thiourea dianion ligands can form two different isomers. This thesis presents evidence that these compounds undergo a solution phase isomerisation process that is due to the initial formation of a kinetically favoured product. There are a number of factors that influence the rate of isomerisation from the kinetically favoured isomer into the thermodynamically favoured isomer. The difference in size between the two substituents is proportional to the difference in energy (ΔG [GPt_{rem}-GPt_{adj}]). The greater this difference in energy the faster the kinetic product transforms into the thermodynamic product in solution. When substituents have similar size differences and therefore small $\Delta G(GPt_{rem}\text{-}GPt_{adj})$ values, the apparent rate of isomerisation slows, in the case of $L_{Php\text{-}tol}$ there was no net isomerisation, and a mixture of both isomers was formed.

Table 6.1 shows the relationship between size difference, $\Delta G(GPt_{rem}\text{-}GPt_{adj})$ and relative rate of isomerisation. Size difference is the relative difference between the R group substituents and the phenyl ring. The Ph group was thought of as a 'control' because it is present in all of the compounds. The rates of isomerisation have not been measured accurately and are only approximate values relative to each other. The mechanism of this isomerisation process is unknown so it was not possible to calculate the rates theoretically as an optimised transition state is required.

Table 6.1 The ΔG (Pt_{rem}-Pt_{adj}) values for each substituent, illustrating how these are approximately related to the rate of isomerisation

R	ΔG kJ mol^{-1}	Rate
Me	31.7	Fastest
Bu^n	23.4	Fast
Pr^n	22.8	Fast
Et	20.8	Fast
Pr^i	11.1	Slow
p-tol	-2.6	0
Bu^t	-30.7	Fastest

From the study of the n-alkyl groups it also became evident that increasing the chain length of a straight chain alkyl does not have a significant impact on the ΔG(GPt_{rem}-GPt_{adj}) beyond 2 carbons. As postulated in Section 3.2 it is the addition of steric bulk around the carbon group adjacent to the nitrogen directly bonded to the platinum that has the greatest effect. This is effectively demonstrated by the branched chain series of Me, Et, Pr^i and Bu^t groups. Each additional CH_3 group increases the steric bulk around the nitrogen adjacent carbon and this effectively decreases the ΔG(GPt_{rem}-GPt_{adj}) value. While there is still at least one H group to orientate towards the bulky PPh_3 group (L_{PhMe}, L_{PhEt}, P_{PhPri}) the Pt_{adj} isomer is still favoured. Once theat H is replaced with a CH_3 (L_{PhBut}) the ΔG(GPt_{rem}-GPt_{adj}) value changes sign and drops significantly, the Pt_{rem} isomer becomes the thermodynamically favoured structure.

To further investigate these compounds and their solution phase isomerism a wider range of groups would be required. A range of alkyl-alkyl, aryl-alkyl, aryl-aryl groups with a wider range of substituent combinations and a selection of other groups, such as CN, OH, CF_3, NH_2 would be highly interesting to investigate. These non-hydrocarbon groups would also provide different electronic environments, which could alter the isomerisation process.

A more accurate determination of the rates of isomerisation would be required. This can be done with the NMR techniques used in this thesis, but the experiments would need to be carried out with a focus on obtaining quantitative kinetic data. DFT calculation can be used to calculate rates of reaction, but this requires the transition state (TS) to calculate activation energies for the isomerisation process. The mechanism by which this isomerisation takes place is currently unknown. With substantially larger computational expense it would be possible to optimise the TS for the isomerisation reaction to better understand the mechanism. There is the potential that sequential 2D NMR techniques could shed light on how the molecule connectivity changes as it isomerises. 2D NMR techniques are notoriously low resolution, and need long experiment times which are not suited to a quickly isomerising compound. Low temperature NMR studies could be used to slow the rate of isomerisation and achieve well resolved spectra.

References

1. Schroeder, D. C. Thioureas. *Chemical Reviews* **1955**, *55*, 181-228.
2. Hebeish, A.; El-Rafie, M. H.; Waly, A.; Moursi, A. Z. Graft copolymerization of vinyl monomers onto modified cotton. IX. Hydrogen peroxide–thiourea dioxide redox system induced grafting of 2-methyl-5-vinylpyridine onto oxidized celluloses. *Journal of Applied Polymer Science* **1978**, *22*, 1853-1866.
3. Services, U. S. D. o. H. a. H. *Report on Carcinogens*; 12th ed.: U.S. Dept. of Health and Human Services, Public Health Service, National Toxicology Program, 2011.
4. Buu-Hoi, N. P.; Xuong, N. D.; Nam, N. H. 423. Potential antiviral thiourea derivatives. *Journal of the Chemical Society (Resumed)* **1956**, 2160-2165.
5. Karakuş, S.; Güniz Küçükgüzel, Ş.; Küçükgüzel, İ.; De Clercq, E.; Pannecouque, C.; Andrei, G.; Snoeck, R.; Şahin, F.; Faruk Bayrak, Ö. Synthesis, antiviral and anticancer activity of some novel thioureas derived from N-(4-nitro-2-phenoxyphenyl)-methanesulfonamide. *European Journal of Medicinal Chemistry* **2009**, *44*, 3591-3595.
6. Asieh Yahyazadeh, Z. G. Synthesis of Unsymmetrical Thiourea Derivatives. *Eur. Chem. Bull* **2013**, *2*, 573-575.
7. Venkatachalam, T. K.; Mao, C.; Uckun, F. M. Effect of stereochemistry on the anti-HIV activity of chiral thiourea compounds. *Bioorganic & Medicinal Chemistry* **2004**, *12*, 4275-4284.
8. Yonova, P. A. S., G M Synthesis and biological activity of urea and thiourea derivatives from 2-aminoheterocyclic compounds: [1]. *Journal of Plant Growth Regulation* **2004**, *23*, 280-291.

9. Yuen, H. Y.; Henderson, W.; Oliver, A. G. Nickel(II) complexes of di- and tri-substituted thiourea mono- and di-anions. *Inorganica Chimica Acta* **2011**, *368*, 1-5.
10. Henderson, W.; Nicholson, B. K.; Dinger, M. B.; Bennett, R. L. Thiourea monoanion and dianion complexes of rhodium(III) and ruthenium(II). *Inorganica Chimica Acta* **2002**, *338*, 210-218.
11. Pearson, R. G. Hard and Soft Acids and Bases. *Journal of the American Chemical Society* **1963**, *85*, 3533-3539.
12. Hartley, F. R. *The Chemistry of Platinum and Palladium*; 1973 ed.; Applied Science Publishers LTD: London, 1973; 544.
13. Henderson, W.; Nicholson, B. K.; Rickard, C. E. F. Platinum(II) complexes of chelating and monodentate thiourea monoanions incorporating chiral, fluorescent or chromophoric groups. *Inorganica Chimica Acta* **2001**, *320*, 101-109.
14. Bierbach, U.; Hambley, T. W.; Roberts, J. D.; Farrell, N. Oxidative Addition of the Dithiobis(formamidinium) Cation to Platinum(II) Chloro Am(m)ine Compounds: Studies on Structure, Spectroscopic Properties, Reactivity, and Cytotoxicity of a New Class of Platinum(IV) Complexes Exhibiting S-Thiourea Coordination. *Inorganic Chemistry* **1996**, *35*, 4865-4872.
15. Braband, H.; Abram, U. Tricarbonyl complexes of rhenium(I) and technetium(I) with thiourea derivatives. *Journal of Organometallic Chemistry* **2004**, *689*, 2066-2072.
16. Okeya, S.; Fujiwara, Y.; Kawashima, S.; Hayashi, Y.; Isobe, K.; Nakamura, Y.; Shimomura, H.; Kushi, Y. Novel Bis(triphenylphosphine)platinum(II) Complexes Containing a Thiourea or

a 1,3-Diethylthiourea Dianion as an N,S-Chelating Ligand. *Chemistry Letters* **1992**, *21*, 1823-1826.

17. Henderson, W.; Kemmitt, R. D. W.; Mason, S.; Moore, M. R.; Fawcett, J.; Russell, D. R. Thiadiazatrimethylenemethane and N,N'-P-triphenylphosphonothioic diamide complexes of platinum(II). *Journal of the Chemical Society, Dalton Transactions* **1992**, 59-66.
18. Henderson, W.; Nicholson, B. K. Synthesis and electrospray mass spectrometry of platinum(II) complexes derived from thiourea dianions and the X-ray structure of [Pt{NMeC(=NCN)S}(COD)] (COD = cyclo-octa-1,5-diene). *Polyhedron* **1996**, *15*, 4015-4024.
19. Pilato, R. S.; Eriksen, K. A.; Stiefel, E. I.; Rheingold, A. L. Generation of Cp_2Mo:S and cycloaddition of the molybdenum sulfido bond with di-p-tolylcarbodiimide. *Inorganic Chemistry* **1993**, *32*, 3799-3800.
20. Henderson, W.; Nicholson, B. K.; Dinger, M. B. Synthesis and crystal structure of the first complex containing a chelating selenourea dianion ligand. *Inorganica Chimica Acta* **2003**, *355*, 428-431.
21. Bodensieck, U.; Carraux, Y.; Stoeckli-Evans, H.; Süss-Fink, G. Tris(N,N′-diphenylthioureato)-chromium(III). *Inorganica Chimica Acta* **1992**, *195*, 135-137.
22. Coles, M. P.; Swenson, D. C.; Jordan, R. F.; Young, V. G. Aluminum Complexes Incorporating Bulky Nitrogen and Sulfur Donor Ligands. *Organometallics* **1998**, *17*, 4042-4048.
23. Alagöz, C.; Brauer, D. J.; Mohr, F. Arene ruthenium metallacycles containing chelating thioamide ligands. *Journal of Organometallic Chemistry* **2009**, *694*, 1283-1288.

24. Robinson, S. D.; Sahajpal, A.; Steed, J. W. N,N′-Diphenylthioureido complexes of ruthenium, osmium and iridium. *Inorganica Chimica Acta* **2000**, *306*, 205-210.
25. Smith, T. S.; Henderson, W.; Nicholson, B. K. Cycloaurated gold(III) complexes with monoanionic thiourea ligands. *Inorganica Chimica Acta* **2013**, *408*, 27-32.
26. Henderson, W.; Rickard, C. E. F. Platinum(II), palladium(II) and gold(III) complexes containing 1,1,4-trisubstituted thiosemicarbazide dianion ligands. *Inorganica Chimica Acta* **2003**, *343*, 74-78.
27. McDermott, J. X.; White, J. F.; Whitesides, G. M. Thermal-decomposition of bis(phosphine)platinum(ii) metallocycles. *Journal of the American Chemical Society* **1976**, *98*, 6521-6528.
28. Frisch, M. J.; Trucks, G. W.; Schlegel, H. B.; Scuseria, G. E.; Robb, M. A.; Cheeseman, J. R.; Scalmani, G.; Barone, V.; Mennucci, B.; Petersson, G. A.; Nakatsuji, H.; Caricato, M.; Li, X.; Hratchian, H. P.; Izmaylov, A. F.; Bloino, J.; Zheng, G.; Sonnenberg, J. L.; Hada, M.; Ehara, M.; Toyota, K.; Fukuda, R.; Hasegawa, J.; Ishida, M.; Nakajima, T.; Honda, Y.; Kitao, O.; Nakai, H.; Vreven, T.; Montgomery, J. A.; Peralta, J. E.; Ogliaro, F.; Bearpark, M.; Heyd, J. J.; Brothers, E.; Kudin, K. N.; Staroverov, V. N.; Kobayashi, R.; Normand, J.; Raghavachari, K.; Rendell, A.; Burant, J. C.; Iyengar, S. S.; Tomasi, J.; Cossi, M.; Rega, N.; Millam, J. M.; Klene, M.; Knox, J. E.; Cross, J. B.; Bakken, V.; Adamo, C.; Jaramillo, J.; Gomperts, R.; Stratmann, R. E.; Yazyev, O.; Austin, A. J.; Cammi, R.; Pomelli, C.; Ochterski, J. W.; Martin, R. L.; Morokuma, K.; Zakrzewski, V. G.; Voth, G. A.; Salvador, P.; Dannenberg, J. J.; Dapprich, S.; Daniels, A. D.; Farkas;

Foresman, J. B.; Ortiz, J. V.; Cioslowski, J.; Fox, D. J. Gaussian 09, Revision B.01. Wallingford CT, 2009.

29. Van Kralingen, C. G.; De Ridder, J. K.; Reedijk, J. Coordination compounds of Pt(II) and Pd(II) with imidazole as a ligand. New synthetic procedures and characterization. *Inorganica Chimica Acta* **1979**, *36*, 69-77.
30. Boere, R. T.; Montgomery, C. D.; Payne, N. C.; Willis, C. J. Complexes of hybrid ligands. Synthesis of a fluoro-alcohol diarylphosphino ligand and its complexes with platinum(2+), palladium(2+), nickel(2+), cobalt(2+), copper(1+), and rhodium(3+): crystal and molecular structure of a trans square-planar nickel(2+) complex with two bidentate ligands showing cis-trans isomerism in solution. *Inorganic Chemistry* **1985**, *24*, 3680-3687.
31. Koo, I.-S. A., Dildar ; Yang, Ki-Yull ; Park, Yong ; Wardlaw, David M. ; Buncel, Erwin Theoretical Study of ^{31}P NMR Chemical Shifts for Organophosphorus Esters, Their Anions and O,O-Dimethylthiophosphorate Anion with Metal Complexes. *Bulletin of the Korean Chemical Society* **2008**, *29*, 2252-2259.

Appendices

Appendix A Method and basis set testing data to support Section 2.1

The following data were collected as part of the research component of module CHEM522-12B Computational Chemistry, completed for the taught component of this MSc.

The DFT functionalstested include B3LYP, M06 and M062x. Each method was tested with a number of basis set combinations to determine the best ratio of cost:accuracy. The combinations are as follows:

- C, H, N, S and P - 6-31G(d)
- C, H - 6-31G(d), N, S, P – 6-31+G(d)
- C, H - 6-31G(d), N, S, P – 6-311++(2d,2p)
- C, H, N, S, P - 6-311++G(2d,2p)

In all causes the LANL2DZ basis set and effective core potential were used for Pt. Table A.1 shows the geometric parameters considered from the crystal structure and the same parameters calculated with each method/basis set combination. The M062X method performed the best regardless of what basis set was used. The 6-31G(d)/6-311++G(2d,2p) basis set combination and the 6-311++G(2d,2p) basis sets performed equally well. For the CHEM522 project, time was a constraining factor, so the 6-31G(d)/6-311++G(2d,2p) basis set combination was used for all calculations as it required under three days to complete calculations. For this thesis, time was not such a large constraint so the larger 6-311++G(2d,2p) basis set, which took approximately 36 days to complete calculations, was used for all calculations involved in this research.

Table A.1 Shows the geometric parameters considered for the method and basis set combinations used

	Pt-N (Å)	Pt-S (Å)	Pt-P1 (Å)	Pt-P2 (Å)	N-Pt-S (^{0})
Expt	2.053	2.332	2.247	2.307	70.5
B3LYP					
6-31G(d)	2.122	2.371	2.339	2.396	69.4
6-31G(d)/6-31+G(d)	2.129	2.368	2.335	2.394	69.3
6-31G(d)/6-311++(2d,2p)	2.119	2.355	2.322	2.386	69.4
M06					
6-31G(d)	2.113	2.363	2.325	2.387	69.6
6-31G(d)/6-31+G(d)	2.117	2.362	2.325	2.380	69.6
6-31G(d)/6-311++(2d,2p)	2.107	2.351	2.315	2.376	69.7
M062X					
6-31G(d)	2.103	2.355	2.276	2.334	69.9
6-31G(d)/6-31+G(d)	2.110	2.350	2.273	2.332	69.9
6-31G(d)/6-311++(2d,2p)	2.103	2.338	2.258	2.319	70.0
6-311++G(2d,2p)	2.108	2.339	2.249	2.311	69.9

Appendix B Representative spectra relating to the n-alkyl substituted thiourea dianion complexes of platinum reported in Section 3.2

This appendix contains spectra images that support the discussion of the n-alkyl substituted thiourea dianion complexes, L_{PhMe}, L_{PhPrn} and L_{PhBun}, in Section 3.2.

As in the main body only the alkyl region is shown for all ^{1}H spectra as the aromatic region is of little interest and complicated by the presence of two PPh_3 groups.

Note: For all spectra a indicated Pt_{adj}, r indicates Pt_{rem} and * indicates unidentified.

B.1 $(Ph_3P)_2PtSC(=NMe)NPh$ (L_{PhMe})

Figure B.1 and Figure B.2 show the ^{1}H NMR spectra during and after the isomerisation process, respectively. The isomerisation of L_{PhMe} is so fast it was not possible to obtain a ^{1}H spectrum of purely the Pt_{rem} isomer.

Figure B.3 shows the ^{31}P spectrum of the compound where the isomerisation process is close to complete. Similarly to the ^{1}H spectrum it was not possible to get a spectrum of the pure Pt_{rem} structure as the complex isomerises too quickly.

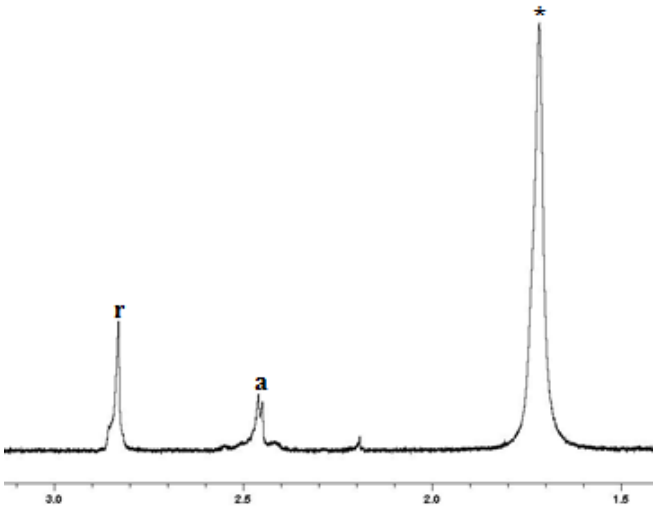

Figure B.1 ^{1}H NMR spectrum of L_{PhMe} before the isomerisation process has completed

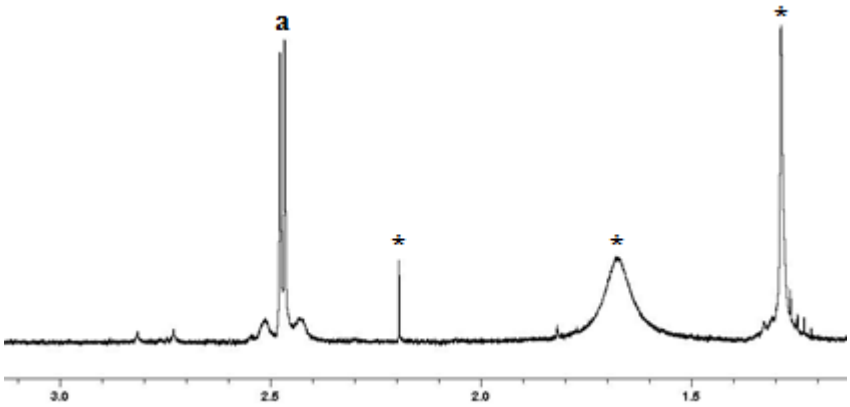

Figure B.2 ^{1}H NMR spectrum of L_{PhMe} after the isomerisation process has completed

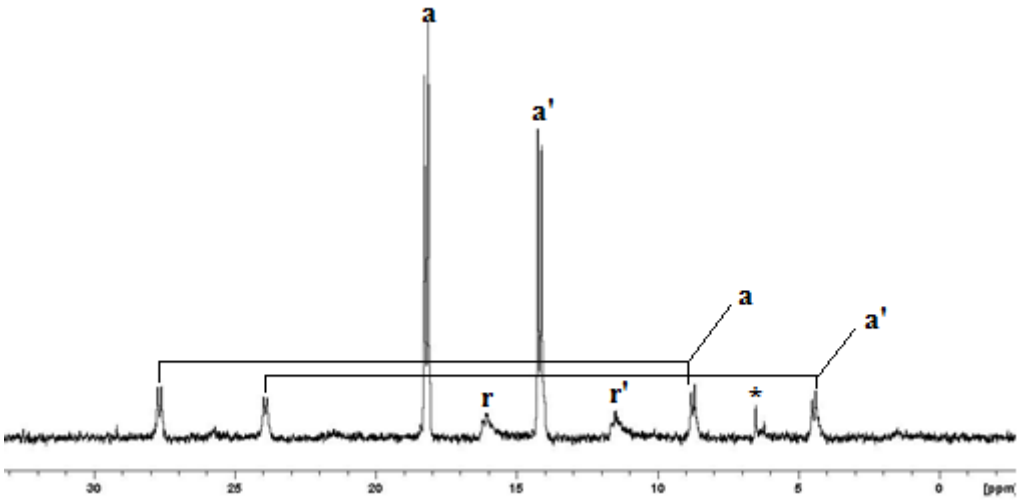

Figure B.3 ^{31}P NMR spectrum of L_{PhMe} before the isomerisation process has completed. Once complete the r and r' signals are no longer visible

B.2 $(Ph_3P)_2PtSC(=NPr^n)NPh$ (L_{PhPrn})

Figure B.4 and Figure B.5 show ^1H NMR spectra of L_{PhPrn} before and after isomerisation is complete. In Figure B.5 platinum coupling is clearly visible on the sides of the multiplet at $\delta \sim 2.8$ ppm.

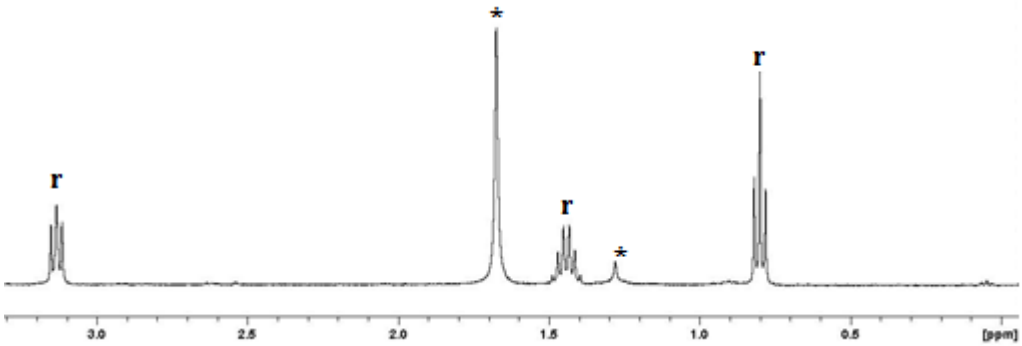

Figure B.4 ^1H NMR spectrum of L_{PhPrn} before the isomerisation process has completed

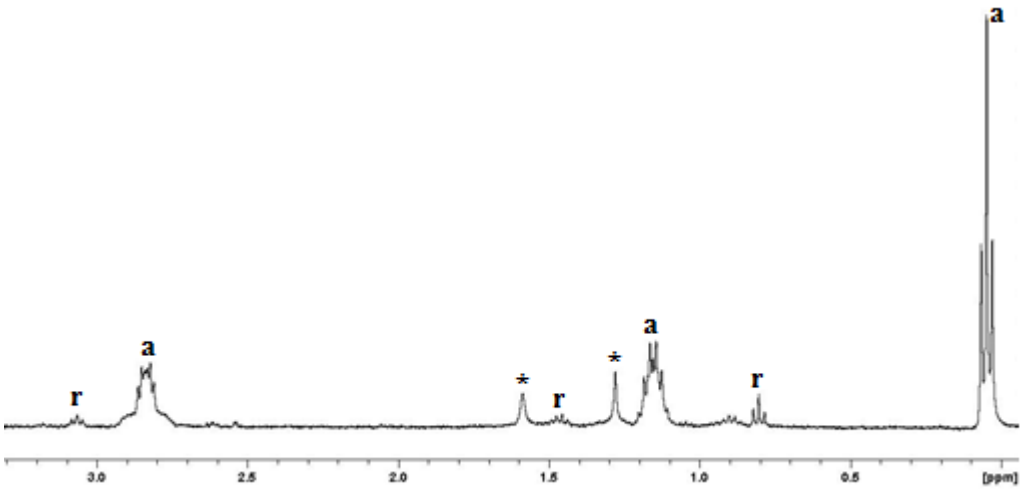

Figure B.5 ^1H NMR spectrum of L_{PhPrn} after the isomerisation process has completed

Figure B.6 and Figure B.7 show the ^{31}P NMR spectra, in Figure B.**6** the Pt_{adj} isomer is just starting to show through downfield of the main signals for the Pt_{rem} isomer.

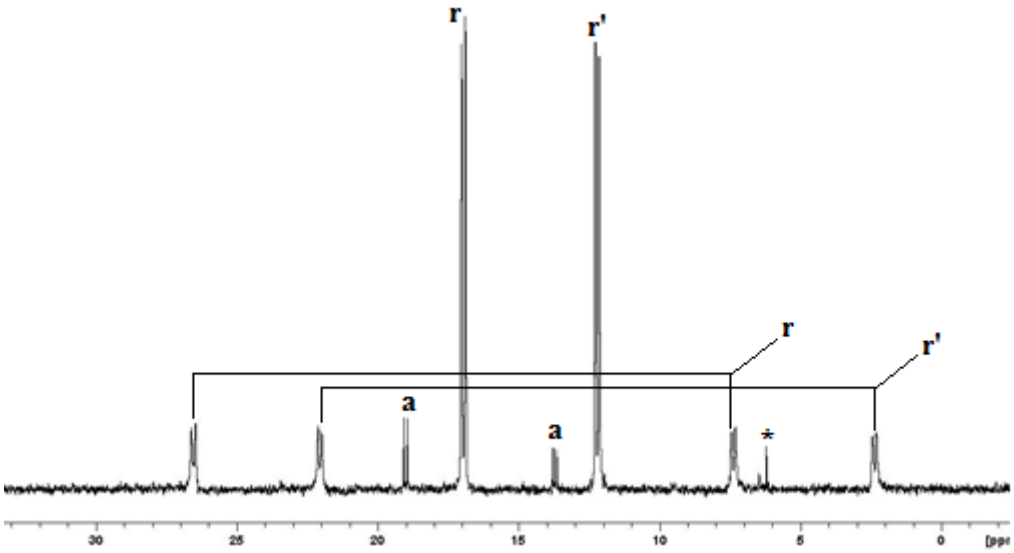

Figure B.6 ^{31}P NMR spectrum of L_{PhPrn} before the isomerisation process has completed

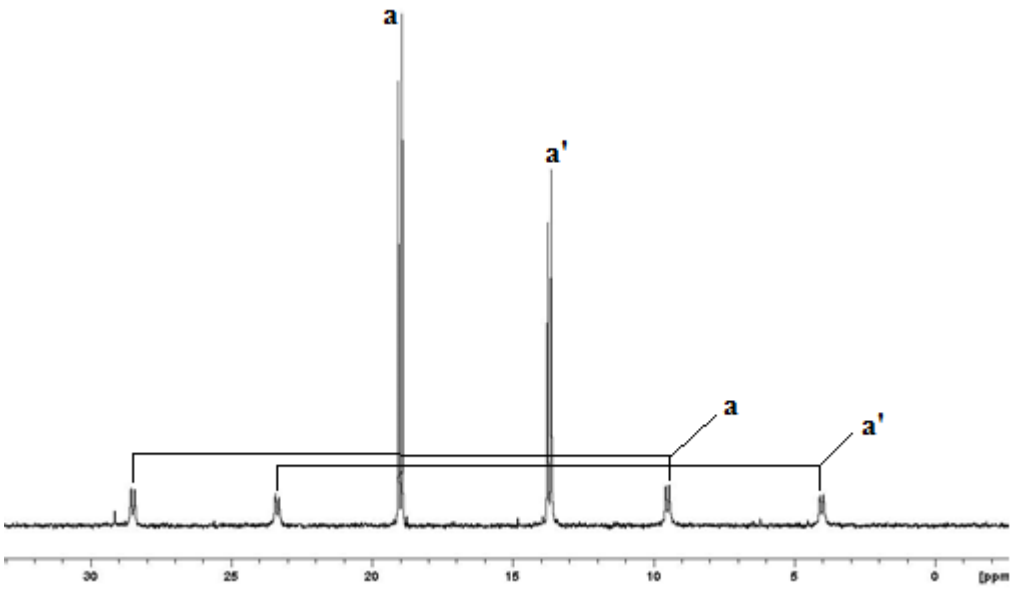

Figure B.7 ^{31}P NMR spectrum of L_{PhPrn} after the isomerisation process has completed

B.3 $(Ph_3P)_2PtSC(=NBu^n)NPh$ (L_{PhBun})

Figure B.8 and Figure B.9 show ^1H NMR spectra of L_{PhBun} before and after isomerisation, due to the long length of the alkyl chain the multiplets between 0.8 and 1.8 ppm do not resolve well and are not assigned to either isomer.

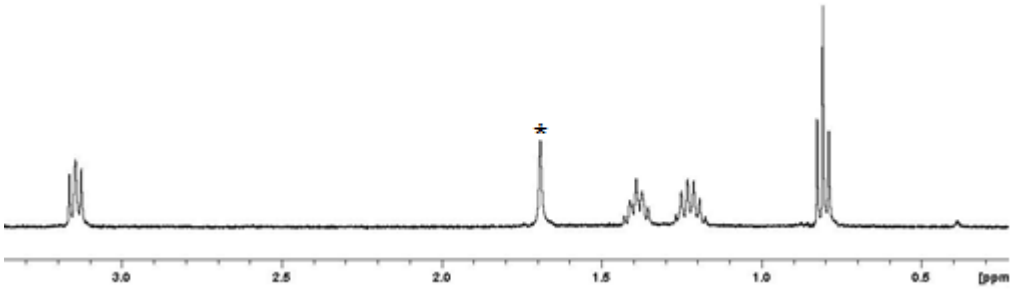

Figure B.8 ^1H NMR spectrum of L_{PhBun} before the isomerisation process has completed

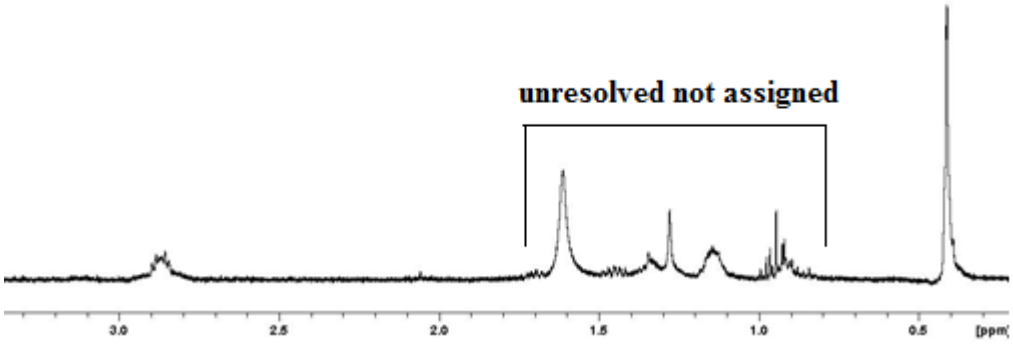

Figure B.9 ^1H NMR spectrum of L_{PhBun} after the isomerisation process has completed

Figure B.10 and Figure B.11 show the ^{31}P NMR spectra of L_{PhBut}, neither shows a pure isomer but they illustrate the change of intensity over time of the two AB pattern signals well.

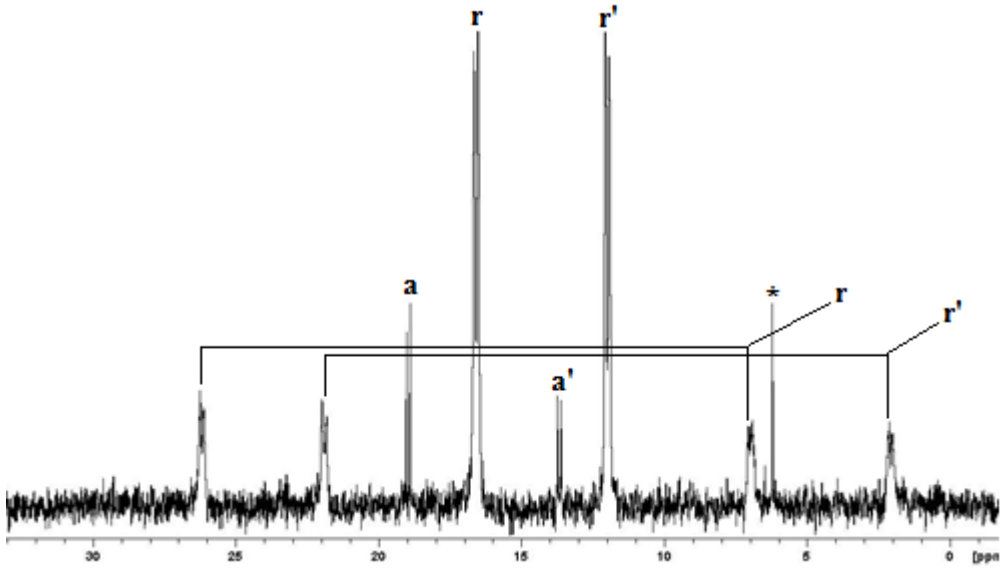

Figure B.10 ^{31}P NMR spectrum of L_{PhBun} as the isomerisation process starts

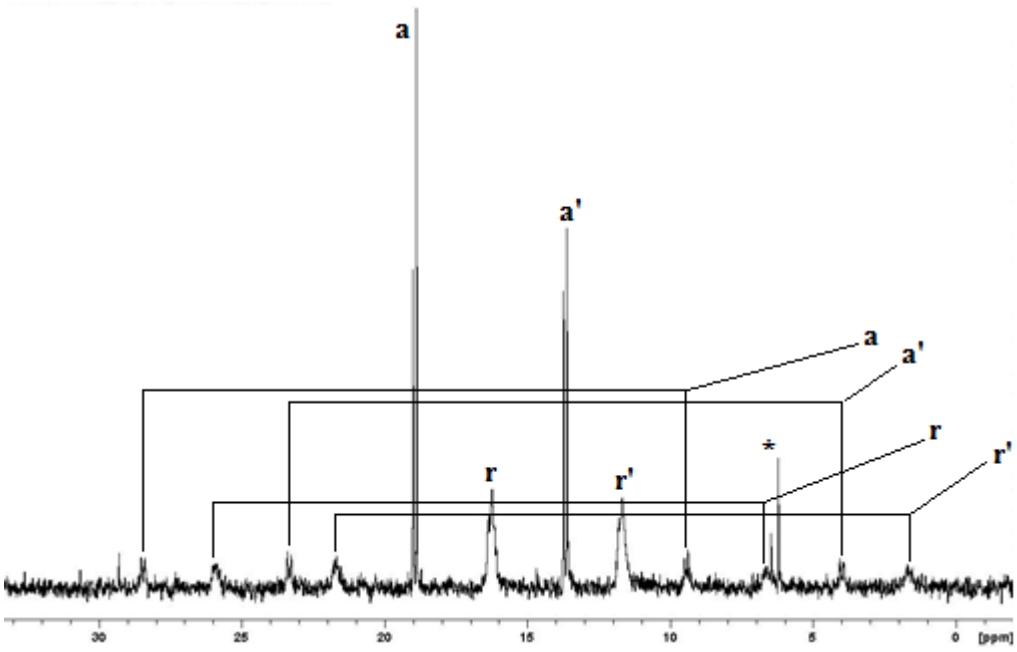

Figure B.11 ^{31}P NMR spectrum of L_{PhBun} nearing the completion of the isomerisation process